HHS Public Access

Author manuscript

Int J Pharm. Author manuscript; available in PMC 2022 September 25.

Published in final edited form as:

Int J Pharm. 2021 September 25; 607: 120943. doi:10.1016/j.ijpharm.2021.120943.

*Corresponding Author: Prof. Mandip Singh, Ph.D., College of Pharmacy and Pharmaceutical Sciences, Florida A&M University, Tallahassee, Florida, 32307, USA, Tel: +1- 850-561-2790 Fax: 850-599-3813; mandip.sachdeva@gmail.com.

†Nilkumar Patel and Nagavendra Kommineni should be considered joint first author.

Author contribution:

Nilkumar Patel

Conceptualization-Lead, Data curation-Lead, Formal analysis-Lead, Funding acquisition-Equal, Investigation-Lead, Methodology-Lead, Project administration-Lead, Resources-Equal, Software-Lead, Supervision-Lead, Validation-Equal, Visualization-Lead, Writing-original draft-Lead, Writing-review & editing-Lead

Nagavendra Kommineni

Conceptualization-Equal, Data curation-Lead, Formal analysis-Lead, Funding acquisition-Equal, Investigation-Lead, Methodology-Lead, Resources-Equal, Software-Lead, Supervision-Lead, Validation-Equal, Visualization-Lead, Writing-original draft-Lead, Writing-review & editing-Lead

Sunil Surapaneni

Conceptualization-Equal, Data curation-Equal, Formal analysis-Equal, Funding acquisition-Equal, Investigation-Lead, Methodology-Equal, Project administration-Equal, Resources-Equal, Software-supporting, Supervision-supporting, Validation- supporting, Visualization- supporting, Writing-original draft- supporting, Writing-review & editing- supporting

Anil Kalavala

Conceptualization-Equal, Data curation-Equal, Formal analysis-Equal, Funding acquisition-Equal, Investigation-Lead, Methodology-Equal, Project administration-Equal, Resources-Equal, Software-Equal, Supervision-Equal, Validation-Equal, Visualization-Equal, Writing-original draft-Equal, Writing-review & editing-Equal

Xuegang Yuan

Conceptualization-Equal, Data curation-Equal, Formal analysis-Equal, Funding acquisition-Equal, Investigation-Lead, Methodology-Equal, Resources-Equal, Software-Equal, Supervision- Equal, Validation- Equal, Visualization- Equal, Writing-original draft- Equal, Writing-review & editing- Equal

Aragaw Gebeyehu

Conceptualization-Equal, Data curation-Equal, Formal analysis-Equal, Funding acquisition-Equal, Investigation-Equal, Methodology-Equal, Project administration-Equal, Resources-Equal, Software-Equal, Supervision-Equal, Validation-Equal, Visualization-Equal, Writing-original draft-Equal, Writing-review & editing-Equal

Peggy Arthur

Conceptualization-Equal, Data curation-Equal, Formal analysis-Equal, Funding acquisition-Equal, Investigation-Equal, Methodology-Equal, Project administration-Equal, Resources-Equal, Software-Equal, Supervision-Equal, Validation-Equal, Visualization-Equal, Writing-original draft-Equal, Writing-review & editing-Equal

Leanne C Duke

Conceptualization-Equal, Data curation-Equal, Formal analysis-Equal, Funding acquisition-Equal, Investigation-Lead, Methodology-Equal, Project administration-Equal, Resources-Equal, Software-Equal, Supervision-Equal, Validation-Equal, Visualization-Equal, Writing-original draft-Equal, Writing-review & editing-Equal

Sara York

Conceptualization-Equal, Data curation-Equal, Formal analysis-Equal, Funding acquisition-Equal, Investigation-Equal, Methodology-Equal, Project administration-Equal, Resources-Equal, Software-Equal, Supervision-Equal, Validation-Equal, Visualization-Equal, Writing-original draft-Equal, Writing-review & editing-Equal

David Meckes Jr

Conceptualization-Equal, Data curation-Equal, Formal analysis-Equal, Funding acquisition-Equal, Investigation-Equal, Methodology-Equal, Project administration-Equal, Resources-Equal, Software-Equal, Supervision-Equal, Validation-Equal, Visualization-Equal, Writing-original draft-Equal, Writing-review & editing-Equal

Mandip Singh

Conceptualization-Equal, Data curation-Equal, Formal analysis-Equal, Funding acquisition-Equal, Investigation-Equal, Methodology-Equal, Project administration-Equal, Resources-Equal, Software-Equal, Supervision-Equal, Validation-Equal, Visualization-Equal, Writing-original draft-Equal, Writing-review & editing-Equal

Declaration of Competing Interest

The authors confirm that there are no competing interests.

Declaration of interests

The authors declare that they have no known competing financial interests or personal relationships that could have appeared to influence the work reported in this paper.

Cannabidiol Loaded Extracellular Vesicles Sensitize Triple-Negative Breast Cancer to Doxorubicin in both *in-vitro* and *in vivo* Models

Nilkumar Patel[1,†], **Nagavendra Kommineni**[1,†], **Sunil Kumar Surapaneni**[1], **Anil Kalvala**[1], **Xuegang Yaun**[3,4], **Aragaw Gebeyehu**[1], **Peggy Arthur**[1], **Leanne C Duke**[2], **Sara B. York**[2], **David G Meckes Jr**[2], **Mandip Singh**[1,*]

[1]College of Pharmacy and Pharmaceutical Sciences, Florida A&M University, Tallahassee, FL, USA.

[2]Department of Biomedical Sciences, Florida State University College of Medicine, 1115 West Call Street, Tallahassee, FL, USA.

[3]Department of Chemical and Biomedical Engineering, Florida State University, Tallahassee, FL, USA.

[4]The National High Magnetic Field Laboratory, Florida State University, Tallahassee, FL, USA.

Abstract

Extracellular Vesicles (EVs) were isolated from human umbilical cord mesenchymal stem cells (hUCMSCs) and were further encapsulated with cannabidiol (CBD) through sonication method (CBD EVs). CBD EVs displayed an average particle size of 114.1±1.02 nm, zeta potential of −30.26±0.12 mV, entrapment efficiency of 92.3±2.21% and stability for several months at 4 °C. CBD release from the EVs was observed as 50.74±2.44% and 53.99±1.4% at pH 6.8 and pH 7.4, respectively after 48 h. Our *in-vitro* studies demonstrated that CBD either alone or in EVs form significantly sensitized MDA-MB-231 cells to doxorubicin (DOX) (*P<0.05). Flow cytometry and migration studies revealed that CBD EVs either alone or in combination with DOX induced G1 phase cell cycle arrest and decreased migration of MDA-MB-231 cells, respectively. CBD EVs and DOX combination significantly reduced tumor burden (***P<0.001) in MDA-MB-231 xenograft tumor model. Western blotting and immunocytochemical analysis demonstrated that CBD EVs and DOX combination decreased the expression of proteins involved in inflammation, metastasis and increased the expression of proteins involved in apoptosis. CBD EVs and DOX combination will have profound clinical significance in not only decreasing the side effects but also increasing the therapeutic efficacy of DOX in TNBC.

Graphical Abstract

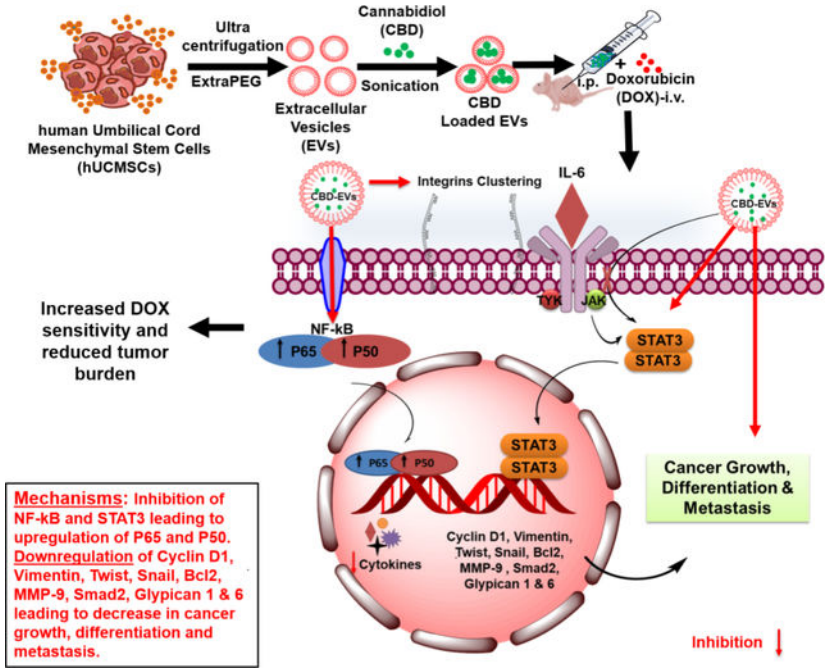

Keywords

Cannabidiol; Extracellular Vesicles; Sensitization; Doxorubicin; Triple Negative Breast Cancer

1. Introduction

Breast cancer (BC) is the second underlying cause of cancer-associated mortality among women and effective therapeutic management of triple negative breast cancer (TNBC; a subtype of basal-like BC) remains as a major clinical challenge due to recurrence and resistance [1–8]. Doxorubicin (DOX) is clinically used for the effective management of TNBC, but resistance remains as a concern due to autophagy, increased levels of ATP-binding cassette transporters and glutathione S-transferase and EMT [9–12]. Despite liposomes have been tried to improve and maximize the clinical efficacy of chemotherapeutic agents for TNBC, certain limitations like high production cost, poor stability and rapid clearance by the phagocytic system due to their recognition as a foreign substance even though they are similar to cell membrane limit their therapeutic usage [13–25]. Therefore, development of novel therapeutic strategies to combat TNBC is an unmet clinical need [26].

Recently, cannabinoids (Δ9-THC and CBD) are gaining enormous interest in cancer due to their potential effects on regulating cancer cell proliferation, metastasis, angiogenesis, and differentiation [27–32]. Accumulating evidence demonstrates the therapeutic efficacy of CBD in preclinical and clinical models of breast cancer [30,33–37]. A recent study by García-Morales et al., has demonstrated that CBD decreased the IL-1β (i.e., an inflammatory cytokine) induced-invasiveness of breast cancer [38]. CBD also induces autophagy, apoptosis, cell cycle arrest, and inhibits the migration, invasion, epithelial to mesenchymal transition

(EMT) and angiogenesis of various tumors [39–42]. Cannabinoids are also used in combination with radiation therapy/anti-cancer drugs for various cancers [43–46].

Excessive first pass metabolism, poor solubility, and increased metabolism by CYP enzymes contribute to poor bioavailability of CBD and limit its clinical usage [47–49]. CBD is a small lipophilic molecule, which gets oxidized in basic media to quinones [50–52]. Epidiolex® (i.e., a cannabidiol medication approved by USFDA to treat seizures) has shown oral bioavailability of only 13–19 % [53–55]. Hence, improvement of oral bioavailability of CBD is a major clinical challenge and an unmet need. To date, various formulation approaches have been tried to overcome the problems of CBD. CBD loaded PLGA nanoparticles demonstrated anti-cancer effects in ovarian cancer by increasing the protein expression of cleaved PARP [56]. CBD loaded microparticles displayed anti-cancer effects and improved the sensitivity of paclitaxel and doxorubicin in breast cancer [57].

Exosomes or small EVs (vesicles of 30–150 nm) are produced by the invagination of endosomal membranes (i.e., multivesicular bodies) and their subsequent fusion with plasma membrane [58]. Larger EVs are shed from the cell surface and called microvesicles. Recently, EVs have gained much attention for their potential use as drug delivery system (DDS) in various diseases [59–61]. Apart from their extraordinary roles in mediating cell-cell communication, EVs (endogenous nanovesicles) are promising drug carriers for both hydrophilic (such as siRNAs and miRNAs) and hydrophobic drugs in cancer because of their high stability and biocompatibility [62,63]. EVs play a crucial role in proliferation, metastasis (EMT), angiogenesis, reprogramming of energy metabolism, immune regulation, transformation of non-neoplastic cells and chemoresistance [64–66]. They also serve as diagnostic/prognostic markers in various cancers [67–69]. Mesenchymal stem cells (MSCs) show their therapeutic effects in various cancers majorly through EVs [70,71]. MSC-derived EVs can encapsulate various cargos (i.e., miRNAs, mRNAs, proteins and drugs), cross the plasma membrane for delivering cargos to their target sites and function either as tumor suppressors/promoters in various cancers depending upon the cell type [72,73].

EVs derived from hUCMSCs (hUCMSCs-EVs) are gaining tremendous attention due to their potential clinical applications in various conditions such as cancer, bronchopulmonary dysplasia, pulmonary hypertension, organ/tissue injury, stroke, liver fibrosis, wound healing, Alzheimer's disease, chronic kidney repair, liver fibrosis, acute inflammation and blood glucose level regulation by shuttling various bioactive components (proteins, lipids, mRNA, miRNA, and DNA) during mediation of cell-cell communication [74–78]. These EVs show their clinical applications in regenerative medicine and serve as potential delivery tools for various chemotherapeutics [79]. Moreover, they have also shown their beneficial effects in peripheral nerve injury models by modulating axonal outgrowth, vascular regeneration and neuroinflammation processes by decreasing inflammatory markers such as TNF-α and IL-1β [80,81]. Meanwhile, clinical applications require large number of cells or EVs, which cannot be manufactured in laboratory. Thus, multiple bioreactors have been designed to improve cell expansion for hMSC based therapy [82,83]. However, EVs production through bioreactors with hMSC culture has not been widely reported as a potential feasible strategy.

As both CBD and hUCMSCs-EVs are well demonstrated in amelioration of cancer, in this study, we hypothesize that therapeutic usage of hUCMSCs-EVs generated from PBS-VW bioreactors would serve as an ideal delivery platform not only for improving the absorption and bioavailability for CBD but also for the reduction of CBD dosage required to achieve tumor regression. To the best of our knowledge, this is the first study demonstrating not only the formulation of CBD loaded EVs by using EVs derived from hUCMSCs but also the therapeutic effects of CBD loaded EVs in TNBC *in-vitro* and *in vivo*. In addition, this study demonstrates the efficacy of CBD EVs in improving the sensitivity of doxorubicin (DOX) in *in-vitro* and *in vivo* models of TNBC.

2. Materials and Methods

2.1 Materials

CBD (GLP and GMP grade) was purchased from Purisys™ (Athens, GA). DOX was purchased from AK Scientific, Inc (Union City, CA). Dulbecco's Modified Eagle Medium (DMEM) and DMEM/Ham's F12 (1:1 Mixture) media were acquired from Millipore Sigma (St. Louis, MO). MDA-MB-231 cells (TNBC) were purchased from ATCC (Rockville, MD, USA). Fetal bovine serum (FBS) was procured from Thomas scientific (Swedesborow, NJ). VitroGel LDP2 hydrogel and Type 1 dilution buffer were received kindly from TheWell Biosciences (NJ, USA). MDA-MB-231 cells were cultured as previously described [84]. Cells were used with passage number below 10. Bovine serum albumin (BSA), sucrose, ethanol, methanol, water (HPLC grade), Triton X-100, formaldehyde, phosphate buffered saline (PBS, 1X) were procured from Sigma Aldrich (St. Louis, MO). Human umbilical cord derived mesenchymal stem/stromal cells (hUCMSCs) of passage 0 to 2 were acquired from the Department of Chemical and Biomedical Engineering, Florida State University. PBS-vertical wheel bioreactor was purchased from PBS Biotech, Inc (Camarillo, CA). Cytodex-1 microcarrier was from VWR International (Radnor, PA). α-MEM medium was purchased from Life Technologies (Carlsbad, CA). Sodium bicarbonate and Penicillin/Streptomycin were procured from ThermoFisher Scientific (Waltham, MA). 150 mm diameter petri dishes are from Corning (Corning, NY, USA). EVs free FBS was used for EVs collection and acquired by ultracentrifugation under 100,000 rcf, 4 °C for 20 h.

2.2 Animals

Female nude mice (5–6 weeks age) obtained from Envigo (Indianapolis, IN) were used for *in vivo* anti-tumor studies. Florida Agricultural and Mechanical University has AAALAC accredited animal facilities, and all the animal experiments carried out were reviewed and approved by the Institutional Animal Use and Care Committee of Florida Agricultural and Mechanical University (protocol number: 020–06) and complied with the NIH guidelines (Guide for the care and use of laboratory animals). All mice were euthanized via exposure to carbon dioxide (CO_2).

3. Methods

3.1 Analytical method for quantification of Cannabidiol (CBD)

The analytical method for CBD was developed by using RP-HPLC (Waters, USA) with a slight modification [85]. Briefly, CBD was dissolved in methanol to obtain a stock solution of 1 mg/mL. A series of standards (0.5, 1, 2, 4, 8, 16 and 32 μg/mL) were prepared. Each Sample of 20 μL was injected and CBD was retained by a Symmerty® C18 column (150×3.9 mm, 5 μm). The mobile phase of methanol: water (85:15 % v/v) was used in an isocratic mode at a flow rate of 1 mL/min. The samples were detected using a Photodiode Array (PDA) detector (waters 2998) with a detection wavelength set at 220 nm.

3.2 Culture of hUCMSCs in PBS-vertical wheel (PBS-VW) bioreactors

hUCMSCs were cultured and expanded up to passage 4 in petri dishes in a standard 5 % CO_2 incubator with EV free complete culture medium (EV free CCM) containing α-MEM with 10 % EV free FBS, sodium bicarbonate and 1 % Penicillin/Streptomycin. Media was changed for every 2–3 days. Cells were grown to 80–90 % confluence and then trypisinized by using 0.25 % trypsin/EDTA to generate single cell suspension for bioreactor culture. Cells were seeded in PBS-VW bioreactor with 0.25 g of Cytodex-1 at the density of 1100–1500 cells/cm^2. During initial seeding phase, medium volume used was 60 mL. The agitation was set to 25 rpm for 5 min and then under static condition for 15 min of 12 cycles for a period of 4 h. After initial seeding, medium volume was adjusted to 100 mL and the agitation speed was set to 25 rpm for further culture. Medium collection was performed every 2 days with 50 % fresh medium change. Sampling of bioreactor was performed every day, and 0.5 mL homogeneous suspension was taken from PBS-VW bioreactor under 25 rpm agitation. Cell morphology and expansion were visualized by Hoechst staining 33342 (Thermofisher) and imaged with an Olympus IX70 microscope using DAPI filter. Medium samples were centrifuged, and supernatant was collected for glucose and lactate measurement. Glucose and lactate concentrations were determined by YSI2950 biochemical analyzer (Yellow Spring, OH).

3.3 Isolation and purification of EVs from cell culture medium

Small EVs were isolated from cell-conditioned medium by modified differential centrifugation using polyethylene glycol (PEG) precipitation/concentration method as earlier described [86–89]. EV pellet suspended in particle free PBS was characterized for NTA (nanoparticle tracking analysis) using ZetaView® BASIC NTA - Nanoparticle Tracking Video Microscope PMX-120, ZetaView software (version 8.05.11 SP4). EVs characterization was performed according to the minimal information for studies of EVs (MISEV) 2018 guidelines issued by the International Society for Extracellular Vesicles [90,91].

3.4 Preparation and optimization of CBD loaded EVs

CBD loaded EVs were prepared by two different methods (incubation and sonication). Briefly, blank EVs (1.5×10^{11} particles/mL) taken in glass vials were added with 10 % w/v sucrose and 0.1 % w/v BSA on an ice bath and were further subjected to mild vortexing in order to dissolve the contents. The above EVs dispersion was incubated at 22/37 °C

with ethanolic CBD at different concentrations (10 % w/w and 20 % w/w as per the protein content in EVs) for 2–3 h. After incubation, the EVs dispersion was evaluated for particle size, particle number and zeta potential by NTA and for free and entrapped CBD content (HPLC analysis). Similarly, CBD loaded EVs were formulated by sonication method using Branson Digital Sonifier 450 (MFG #100–132-888R), where blank EVs (1.5×10^{11} particles/mL) were incubated with CBD solution (10 %, and 20 % w/w as per the protein content) and subjected to different sonication cycles (10–30 % Amplitude, 3 cycles of 30 s on/off for 2 min, 5 min-cooling between each cycle) at different buffer pH conditions (PBS-6.8 and 7.4 with and without 0.1 % (w/v) BSA along with 10 % sucrose solution) to get final optimized CBD loaded EVs. The obtained formulations were evaluated for physical appearance in terms of precipitation/aggregation, particle size, particle number, zeta potential by NTA and free and encapsulated CBD.

3.5 Characterization of EVs

3.5.1 Particle size and Zeta potential—Average particle size (z-average) and zeta potential of CBD encapsulated EVs were analyzed by dynamic light scattering (DLS) technique at 25 °C with 90° scattering angle using NTA and Zeta View instrument (ZetaView® TWIN PMX-220) and the data was processed using ZetaView Analysis software as previously described [92]. All the prepared EVs were diluted with particle free PBS at 1:1000 dilution and measured in triplicate.

3.5.2 Morphological examination of CBD loaded EVs by TEM—The surface morphology of EVs were determined by Electron microscopy imaging according to the method as described by Lasser et al [93]. EVs protein content was estimated by using Pierce™ BCA Protein Assay Kit - Reducing Agent Compatible.

3.5.3 Drug loading and entrapment efficiency—Theoretical CBD loading was varied from 10–20 % w/w for EVs. CBD present in EVs (entrapment efficiency) was determined by an ultrafiltration method using Vivaspin® 500 centrifugal filter unit (Sartorius, USA) followed by RP-HPLC analysis as per earlier report [94]. The percentage entrapment efficiency (% EE) was calculated by using Eq-1.

$$\%\mathrm{EE} = \frac{\text{Amount of drug entrapped}}{\text{Total amount of drug taken}} X 100 \qquad \text{Eq-1}$$

3.5.4 *In-vitro* CBD release from EVs—*In-vitro* drug release study was performed by a modified dialysis bag method as per earlier report [95–97]. CBD loaded EVs dispersion (100 μg/mL) was sealed in a preactivated dialysis membrane pouch with molecular weight cut off (MWCO) of 12 kDa (Sigma-Aldrich, MO) and placed in 10 mL of release media (PBS, pH (6.8 and 7.4) containing 0.5 % tween 80) present in closed glass tubing which was kept in shaker bath (120 rpm at 37 °C). At predefined time intervals, sample of 1 mL was withdrawn, replaced with fresh medium to maintain sink condition and analyzed for CBD content by RP-HPLC.

3.5.5 Stability studies—The optimized CBD loaded EVs were stored at 4 / 5±3 °C for 1 month and checked for particle size, zeta potential, and particle number by NTA and free and encapsulated CBD content was analyzed by HPLC method as described above.

3.6 Cell viability assay

MDA-MB-231 cells seeded in 96 well plates (6×10^3 cells/well) were treated with various concentrations of blank EVs, DOX, CBD and CBD EVs (0.1–10 μM) for 48 h. In another set of experiments, we performed cytotoxicity assay by using 1 μM CBD and 1 μM CBD EVs as a chemosensitizer for 24 h and followed by 48 h treatment with DOX (0.1–10 μM) followed by MTT staining as previously described [16].

3.6.1 3D cell cultures and cytotoxic assay—The cytotoxic effects of CBD and CBD EVs in 3D non-printed cultures of MDA-MB-231 cells were evaluated according to the methods as described earlier [16]. After the fifth day of spheroids formation, cells were treated with different concentrations of CBD and CBD EVs for 48 h. Viability of the cells was determined using MTT assay.

3.6.2 Cell and tumor uptake studies for fluorescent EVs—Cell uptake studies were performed to evaluate the cell permeation ability of fluorescent EVs. Briefly, cells were seeded in a 6 well plate (5000 cells/well), incubated for 24 h and treated with fluorescent EVs (SYTO® RNASelect™ Green Fluorescent Cell Stain (S32703) Invitrogen™ Van Allen Way, Carlsbad, CA) for 48 h. Afterwards cells were washed thrice with PBS and fixed with 4 % v/v paraformaldehyde solution. 4, 6-diamidino-2-phenylindole (DAPI) was used for nuclei staining. Similarly, 100 μL of fluorescently labelled EVs were injected to mice by i.p. and after 5 h, the animal was sacrificed, and MDA-MB-231 tumor tissue was isolated. The isolated tissue was washed thoroughly in PBS and then 10-micron sections were prepared using a Cryotome (Shandon). The processed sections were stained with DAPI solution. Confocal laser scanning microscope (Leica TCS SP8 Laser Scanning Spectral Confocal Microscope) was used for capturing fluorescent images at 400x magnification.

3.6.3 Cell cycle analysis—MDA-MB-231 cells were seeded in 6 well plates (5×10^5 cells per well) and allowed to grow to 70–80 % confluency. Media was removed from the wells and after washing twice with PBS, the cells were treated with CBD, CBD EVs (1, 2.5, 5 μM) for 48 h. In another set, the cells were pre-sensitized with CBD and CBD EVs for 24 h followed by treatment with DOX (500 nM) for 48 h. After treatment, media was removed and the cells were washed twice with PBS, trypsinized by using 0.25 % trypsin-EDTA, centrifuged at 300 × g for 8–10 min and then the supernatant was removed. Fixation of the cells was carried out by using ice-cold 70 % v/v ethanol overnight at 4°C. The suspension was centrifuged at 300 × g for 8–10 min and the supernatant was removed. The obtained cell pellet was resuspended in PBS and centrifuged at 300 × g for 8–10 min. Then the cells were treated with 100 μg/mL of RNase A for 30 min and suspended in 1 mL of propidium iodide (PI) staining buffer containing 50 μg/mL concentration of PI. The suspension was incubated in the dark for 30 min at room temperature and subsequently analyzed for DNA using BD FACS Calibur flow cytometer (BD Bioscience, Franklin Lakes, NJ). The percentage of

cell-cycle distribution in G0/G1, S and G2/M phases of the cell cycle were quantified by using Flow Jo software version 7.6.1.

3.6.4 Cell migration assay—MDA-MB-231 cells were dissociated by using 0.25 % Trypsin-EDTA (Sigma) and seeded into the upper chamber of CIM-16 plates (40000 cells/well) in DMEM serum free medium. DMEM medium supplemented with 1 % FBS was added into the lower chamber as a chemoattractant. Impedance background measurement was initially assessed by adding 50 μL of cell culture medium into each well of the CIM-16 plate. CBD EVs (1 μM), DOX (500 nM) and CBD (1 μM) + DOX (500 nM) combination treatments were used in our study. A minimum of 4 wells per sample were placed according to the manufacturer's instructions and readings were taken every 10 min for a period of 40 h in xCELLigence label-free RTCA (real-time cell analysis) DP instrument (ACEA Biosciences, San Diego, CA, USA). The continuous and automatic electronic readout of cell–sensor impedance is displayed in real-time as Cell Index (a.u), a value which varies depending on the number of migrated cells into the lower chamber over the duration of Time (h).

3.6.5 Immunofluorescence and Confocal Microscopy—Immunocytochemistry was performed according to the methods as described earlier [98–100]. After fixation and permeabilization, the cells were incubated with 3 % w/v BSA for 1 h at room temperature followed by staining with STAT-3 (anti rabbit), p-STAT3 (anti mouse) and anti-rabbit SP-1 (Cell Signalling Technologies, USA) for overnight at 4 °C by diluting the primary antibodies (1:100) in 3 % w/v BSA solution. Later, cells were washed thrice with PBST and then incubated with FITC conjugated anti-mouse secondary antibody (1:200 dilution) or red conjugated secondary antibody (Santa Cruz Biotechnology Inc., CA, USA; 1:100 dilution) for 2 h in the dark at room temperature. Then, the cells were washed thrice with PBST and cover slips were finally mounted with NucBlue™ (ThermoFischer, USA) on a glass slide. Slides were subjected to confocal imaging using a confocal microscope (Leica TCS SP8 Laser Scanning Spectral Confocal).

3.7 Anti-tumor studies in TNBC athymic nude mice

MDA-MB-231 cells xeno-transplanted breast cancer model was used to evaluate the chemo sensitization effect of CBD and CBD EVs in combination with DOX. MDA-MB-231 cells (2.5 million in 100 μL of matrigel) were injected subcutaneously in nude mice and allowed to reach the tumor volume of 1000–1500 mm^3. Animals were then subjected to randomized grouping (4 animals per each group) before treatment (Control, EVs, CBD, CBD EVs, CBD + DOX, CBD EVs + DOX). Animals were administered with CBD (5 mg/kg), EVs ($\approx 10^{10}$/mice), CBD EVs (5 mg/kg) by i.p route. However, in combination study CBD and CBD EVs were administered one day before the dosing of DOX (2 mg/kg, i.v.) to evaluate the chemosensitization effect. The treatment was continued for 2 weeks with twice a week treatment schedule. The tumor volume was measured periodically using vernier caliper and the tumor volumes were calculated by the formula Tumor volume=1/2 xy^2, where 'x' and 'y' represent the length and width of the tumors. The animals were euthanized, tumors were collected and processed for further analysis.

3.8 Immunoblotting

Tissue and cell proteins were extracted by using radioimmunoprecipitation assay (RIPA) lysis buffer to perform western blotting as reported earlier [16,101]. Protein estimation was performed by using BCA Protein Assay Reagent kit. Equal concentration of protein was loaded and performed SDS PAGE gel electrophoresis and then electrophoretically transferred onto PVDF membrane by using Trans-Blot® Turbo™ Transfer System (Bio-Rad). Afterwards, the membrane was subjected to blocking for 1 h at room temperature by using PBS containing 0.1 % Tween 20 and 3 % w/v BSA. The membrane was incubated with primary antibodies {IL-17 (rabbit, 1:1000, Catalog no: 13838S, Cell Signaling Technology, USA), β-actin (rabbit, 1:1000, Catalog no: 4970S, Cell Signaling Technology, USA), NF-κB (rabbit, 1:1000, Catalog no: 8242S, Cell Signaling Technology, USA), Twist (rabbit, 1:1000, Catalog no: 69366S, Cell Signaling Technology, USA), STAT3 (rabbit, 1:1000, Catalog no: 12640S, Cell Signaling Technology, USA), p-STAT3 (mouse, 1:1000, Catalog no: SC-8059, Santa Cruz Biotechnology, USA), BAX (rabbit, 1:1000, Catalog no: 5023, Cell Signaling Technology, USA), Bcl2 (rabbit, 1:1000, Catalog no: 3498S, Cell Signaling Technology, USA), Cleaved Cas-3 (rabbit, 1:1000, Catalog no: 9661, Cell Signaling Technology), Integrin α−5 (rabbit, 1:1000, Catalog no: 4705T, Cell Signaling Technology, USA), TGF-β (rabbit, 1:1000, Catalog no: 3709, Cell Signaling Technology, USA), IL-6 (rabbit, 1:1000, Catalog no: 12153, Cell Signaling Technology, USA), Caspase-9 (rabbit, 1:1000, Catalog no: 9508, Cell Signaling Technology, USA), m-Tor (rabbit, 1:1000, Catalog no: 2983, Cell Signaling Technology, USA), GPC1 (rabbit, 1:1000, Catalog no: SAB1303133, Sigma-Aldrich, USA), GPC6 (rabbit, 1:1000, Catalog no: SAB1303579, Sigma-Aldrich, USA)} for overnight at 4°C. The blots were washed thrice with PBS containing 0.1 % Tween-20 (PBST)) for 5 min each time, incubated with appropriate HRP-conjugated secondary antibodies {rabbit anti-mouse IgG (catalog number: 7076S; Cell Signaling Technology, USA); goat anti-rabbit IgG (catalog number: 7074S; Cell Signaling Technology, USA)} for 1 h room temperature followed by washing thrice with PBST for 5 min each time. The blots were incubated with Super Signal West Pico Chemiluminescent substrate and their images were captured using Chemidoc Instrument (Bio-Rad). The immunoblots were quantified by densitometry scanning using NIH ImageJ software (1.43u; https://imagej.nih.gov/ij).

3.9 HPLC Analysis

RP-HPLC method was developed for CBD and the retention time was observed to be 3.53 min. The calibration curve (average peak area vs concentration) generated over the range of 0.1–32 μg/mL was found to be linear with a correlation coefficient of 0.9995, slope (78147), intercept (5548).

3.10 Statistical analysis

The values were represented as mean ± SEM. The intergroup variations were measured by two tailed student's t-test or one-way ANOVA followed by "Bonferroni's Multiple Comparison Test" using the Graph Pad Prism, version 5.01. Results with p values <0.05 were statistically significant.

4. Results

4.1 hUCMSCs growth and expansion in PBS-VW bioreactor

hUCMSCs were expanded in 2D planar culture and seeded in a microcarrier based, suspension culture system as PBS-VW bioreactor. As shown in Figure 1A, initial seeding confirmed microscopically for 5–10 cells/microcarrier. hUCMSCs cell growth was also visualized in our study. Media samples were subjected to estimation of glucose and lactate concentrations, and we observed active metabolism of cells when they are grown in the PBS-VW bioreactors (Figure 1B). Interestingly, glucose/lactate yield remained consistent at approximately 1.2, indicating that majority of the energy metabolism of hUCMSCs was relied on glycolysis in the PBS-VW bioreactor system (Figure 1C).

4.2 Characterization of EVs derived from human umbilical cord mesenchymal stem cells (hUCMSCs-EVs)

EVs were successfully isolated from different sources of media collected upon growing hUCMSCs in various conditions through differential centrifugation using extra-PEG precipitation technique. The isolated EVs were characterized by NTA for average particle size, particle number as well as zeta potential. The mean particle size of EVs collected from hUCMSCs grown in petri dishes was found to be 144.75±5.12 nm with an average particle number of 6.8×10^{10} particles/mL, and zeta potential of −58.98±4.56 mV. The average estimated protein content by BCA assay kit was found to be 199.46 μg/mL. In the next set of experiments, hUCMSCs were grown in multilayer flask and the isolation of EVs from the supernatant media was carried out by differential centrifugation method. The mean particle size of isolated EVs was found to be 153.2±4.7 nm, with an average particle number of 2×10^{11} particles/mL, zeta potential of −70.38±0.25 mV and the estimated protein content of 936 μg/mL. Electron microscopy was performed to confirm the presence of EVs. hUCMSCs-EVs and hUCMSCs-CBD EVs were observed to be small round particles with typical cup-shaped morphology (Figure 1E). In addition, 0.1 Liter PBS-VW bioreactor was used to scaleup the EVs. Here, we used Cytodex 1 microcarriers, a support matrix which facilitates the growth of hUCMSCs in a bioreactor and allows culturing the cells for 1 week. The isolated media from the bioreactor was processed for differential centrifugation using PEG as a precipitating agent to enrich for EVs. The final recovered EVs were found with an average particle size of 152.1±3.2 nm, particle number (1.5×10^{16} particles/mL), average protein concentration (2.32 mg/mL), and zeta potential of −38.61±0.01 mV.

4.3 Preparation and optimization of CBD loaded EVs

Initially CBD loaded EVs were formulated by simple incubation method. After loading of CBD into EVs, the free drug was removed by dialysis method as per earlier reports [102]. The average particle size was found to be 125.48±5.12 nm with an entrapment efficiency of 70.23±3.24 % CBD (100 μg is equivalent to 10 % drug loading according to the protein concentration) and zeta potential of −40.39±0.12 mV and the average particle number (1.2×10^{11} particles/mL). Alternatively, sonication was used to load CBD into EVs, and different parameters were optimized as mentioned in table 1. The prepared CBD loaded EVs formulations were stored at 4 °C to check the stability in terms of physical appearance, particle size, zeta potential and particle number. The final optimized formulation parameters

were observed to be: PBS with 0.1 % (w/v) bovine serum albumin (BSA) pH 7.4, 10 % w/w sucrose, with sonication conditions (20 % Amplitude (Amp), 3 cycles of 30 s on/off for a total of 2 min with a 5 min-cooling period between each cycle), followed by incubation at 22/37 °C for 1 h. Herein, EVs with 10 % CBD loading was observed with an average particle size of 114.1±1.02 nm (Figure 1D) and entrapment efficiency of 92.3±2.21 % and zeta potential of −30.26±0.12 mV. Before sonication, the size of EVs were found to be 146.43±2.12 nm, with a zeta potential of −42.29±0.32 mV. However, in other conditions there was a rapid precipitation and settling of protein was observed upon storage. At 20 % drug loading, precipitation of CBD as crystals was observed in the dispersion. The final optimized CBD EVs formulations were stored at 4 °C and monitored for particle size and entrapment efficiency. After 1 month, we observed slight decrease in the particle size (109.8 ± 0.98 nm) with an entrapment efficiency of 91.31±1.32 % and zeta potential of −32.48±0.12 mV.

4.4 *In vitro* drug release from CBD loaded EVs:

In vitro drug release testing for CBD loaded EVs (100 μg/mL) was performed by dialysis method using cellulose acetate dialysis tubing at different pH conditions (6.8 and 7.4) in PBS. Sustained CBD release was observed from EVs at both pH conditions. The percent cumulative CBD release was found to be 50.74±2.44 % at pH 6.8 after 24 h, however at pH 7.4 the percent cumulative CBD released was observed to be 53.99±1.4 % as shown in Figure 1G.

4.5 Effect of CBD EVs on cell viability

Cell viability assays were performed for CBD, blank EVs, CBD EVs, DOX against MDA-MB-231 cell line from 0.156 to 10 μM concentrations and the IC_{50} values are represented in (Figure 2). CBD and CBD EVs with 1 μM concentration was selected to check the chemo sensitization effect in combination with DOX. MDA-MB-231 cells treated with blank EVs showed an average cell death of 20–25 %. CBD alone showed IC_{50} values of 3.72 μM (Figure 2A) and 23.66 μM (Figure 2E) in 2D and 3D cultures of MDA-MB-231 cells, respectively. However, CBD EVs showed IC_{50} values of 3.01 μM (Figure 2D) and 21.96 μM in 2D and 3D cultures of MDA-MB-231 cells, respectively. MDA-MB-231 cells sensitized with 1 μM concentration of CBD and CBD EVs for 24 h, followed by treatment with different concentrations of DOX for 48 h resulted in DOX IC_{50} values of 2.4 μM (Figure 2F) and 2.37 μM (Figure 2G) respectively.

4.6 Cell cycle analysis

Flow cytometry of cell cycle analysis was performed after treating MDA-MB-231 cells with 5 different treatments [CBD (1 μM), CBD EVs (1 μM), DOX (500 nM), CBD (1 μM) + DOX (500 nM) and CBD EVs (1 μM) + DOX (500 nM)] to study the distribution of cells in different phases (G1, S and G2) and to detect the apoptotic cells with fractional DNA content. Both CBD EVs (1 μM) and CBD EVs (1 μM) + DOX (500 nM) combination significantly (**P<0.01 & ***P<0.001) increased the cell population in sub G1 phase when compared to control groups (Figure 3A–G). Additionally, DOX (500 nM) alone and CBD (1 μM) + DOX (500 nM) combination treatment significantly (*P<0.05) increased the

percentage of cells in G1 phase when compared to control group, indicating that the cells are undergoing apoptosis.

4.7 Effect of CBD EVs on expression of proteins involved in Inflammation, Metastasis and Apoptosis in MDA-MB 231 cells:

Inflammation and metastasis play an important role in evading immune system surveillance and showing resistance to chemotherapy given for eradicating cancer cells as observed by increased expression of proteins involved in those processes by activating pro-survival strategies [103]. Western blot analysis data revealed that CBD EVs (1 μM) significantly decreased the expression of NF-κB, p-STAT3, STAT3, IL-17 and Twist proteins when compared to free CBD (1 μM & 2.5 μM) and control groups (Figure 4A). Further, we also evaluated the effect of CBD and CBD EVs in improving the sensitivity of DOX by pre-treating MDA-MB 231 cells with CBD (1 μM) and CBD EVs (1 μM) for 24 h followed by treatment with DOX (500 nM) for 48 h. It was observed that CBD EVs (1 μM) + DOX (500 nM) combination significantly decreased the protein expression of NF-κB, p-STAT3, STAT3, IL-17, Bcl2 proteins and increased the expression of BAX protein when compared to control, DOX (500 nM) and CBD (1 μM) + DOX (500 nM) (Figure 4B). These findings were further validated by immunocytochemistry staining which confirmed that CBD EVs (1 μM) + DOX (500 nM) decreased the expression of STAT3, p-STAT3, NF-κB and ITGA5 in MDA-MB-231 cells when compared to other groups (Figures 5A, 5B & 5C). This suggests that CBD EVs either treated alone or in combination with DOX not only decreased the inflammation and metastasis but also facilitated apoptosis of MDA-MB-231 cells.

4.8 Effect CBD EVs in MDA-MB-231 xenograft model of Triple-Negative Breast Cancer

Female Envigo nude mice were used to study the effect of blank EVs (≈ 10^{10}/mice; i.p), CBD (10 mg/kg; i.p), CBD EVs (5 mg/kg; i.p), DOX (2 mg/kg; i.v), CBD (5 mg/kg; i.p) + DOX (2 mg/kg; i.v), CBD EVs (5 mg/kg; i.p) + DOX (2 mg/kg; i.v) on tumor volume at different days of treatment and were compared with control group. We observed after 1st day of treatment, there was no significant difference in tumor volumes of different groups. However, on 4th day of treatment, there was a slight difference in tumor volumes between the groups and the difference was significant as compared to control for CBD (10 mg/kg; *P<0.05), CBD EVs (5 mg/kg; *P<0.05), DOX (2 mg/kg; **P<0.01). Here, pre-sensitization with CBD EVs (5 mg/kg) significantly enhanced anti-tumor effect of DOX (2 mg/kg; **P<0.01). Similarly, at 10th day of treatment, DOX (2 mg/kg; **P<0.01) and combination groups, CBD + DOX (**P<0.01) and CBD EVs + DOX (***P<0.001) predominantly reduced the tumor burden in nude mice when compared to control group. After 2 weeks of treatment, CBD (**P<0.01), CBD EVs (**P<0.01) and DOX (***P<0.001) significantly reduced the tumor volume in nude mice as compared to control (Figure 6A). It was observed that EVs treatment alone has not induced any significant reduction in tumor volume when compared to control group. We observed that pre-sensitization of tumors with CBD (***P<0.001) and CBD EVs (***P<0.001) helped in reducing tumor volume by enhancing DOX uptake. From the above findings, we clearly observed that CBD EVs even at a dose of 5 mg/kg could reduce the tumor burden in TNBC nude mice model as compared to double the dose of free CBD treatment group. These findings were further supported by

Fluorescent EVs uptake study in nude mice with MDA-MB-231 tumors. We observed high fluorescence intensity in the EVs treated tumor tissues (Figure 6B).

4.9 Effect of CBD EVs on Apoptotic and Inflammatory markers in MDA-MB-231 Triple-Negative Breast Cancer Xenograft Model

A variety of cytokines such as IL-6 and TGF-β play an important role in the process of inflammation and almost all of them make a network between tumor microenvironment (TME) and cancer cells, which further suppresses the immune response against tumor [104,105]. We have also evaluated the expression of proteins involved in NF-κB pathway in MDA-MB-231 tumor protein lysate. It was observed that CBD EVs (5 mg/kg) significantly decreased the expression of NF-κB and IL-17 when compared to control group (Figure 7A). In addition, we noticed that CBD EVs (5 mg/kg) induced apoptosis by increasing the expression of Cleaved caspase-3 and BAX and decreasing the expression of Bcl2 respectively (Figure 7A). Moreover, we observed that CBD EVs improved the sensitivity of DOX (western blot analysis of tumor protein lysate), which showed that CBD EVs (5 mg/kg) + DOX (2 mg/kg) combination significantly decreased the protein expression of IL-6, TGF-β and NF-κB when compared to control (untreated) group (Figure 7B). Significant down regulation of Bcl2, mTOR and upregulation of BAX, cleaved caspase-3, and caspase-9 were also observed in CBD EVs (5 mg/kg) + DOX (2 mg/kg) treated tumors when compared to Control, DOX (2 mg/kg) and CBD (5 mg/kg) + DOX (2 mg/kg) group (Figure 7B).

4.10 CBD EVs formulation increased the sensitivity of DOX to reduce metastasis in MDA-MB-231 Triple-Negative Breast Cancer Xenograft Model and MDA-MB-231 cells

Migration, invasion and metabolism can determine the extent of metastasis of cancer cells. It is well known that CBD play an important role in modulation of TME [35]. To investigate the role of CBD EVs formulation in improving the sensitivity to DOX, we have evaluated the expression of proteins which are involved in metastasis by using tumor protein lysate. It was observed that CBD EVs (5 mg/kg) and DOX (2 mg/kg) significantly reduced the expression of Integrin α−5 (ITGA5), Twist, Glypican-1(GPC1), Glypican-6(GPC6) and Smad-2 in comparison to DOX (2 mg/kg), Control and CBD (5 mg/kg) + DOX (2 mg/kg) group (Figure 8A). We also assessed the effect of CBD EVs (1 μM) + DOX (500 nM) combination on the migration of MDA-MB-231 cells by using label-free real-time cell analysis platform (xCELLigence), which monitors the migration of cells for a period of 40 h. It was observed that CBD EVs (1 μM) + DOX (500 nM) combination effectively decreased the migration of MDA-MB-231 cells when compared to control and other treatment groups (Figure 8B).

5. Discussion and conclusions

5.1 Discussion

TNBC is the most prevalent form of malignancy and the leading cause of cancer related deaths in women in western world [106]. Breast cancer associated deaths are due to metastasis of cancer cells to distant organs (i.e., lung, lymph nodes and bone), and chemotherapeutic drug resistance [107,108]. Despite the advances in chemotherapy for the management and prevention of TNBC progression, resistance and recurrence remains as major clinical

concerns [4,109]. Effective treatment strategies are necessary to eradicate drug resistance and deliver payload to the site of action in a tumor microenvironment. Trodelvy (sacituzumab govitecan-hziy), a monoclonal antibody, has been recently approved as a targeted (Trop-2 protein) precision medicine for metastatic TNBC [110]. Therapeutic potential of cannabinoids (Δ9-THC, Δ8-THC and CBD) is well demonstrated in lung cancer, glioma, leukemia, neuroblastoma, skin, uterus, breast, gastric, colorectal, pancreatic, and prostate carcinomas [42]. CBD, a phytocannabinoid from Hemp (*Cannabis sativa*) induces autophagy, apoptosis [111], cell cycle arrest and inhibits the migration, invasion, epithelial to mesenchymal transition (EMT) and angiogenesis of various tumors by acting on CB1 and CB2 receptors, and TRPV1 ion channels and regulating ERK, MAPK, PI3K, p38, AKT and ceramide signaling pathways [112,113]. CBD interacts with G-protein-coupled receptors (Gi/o) and regulates various cellular signaling pathways by inhibition of adenylyl cyclase [114]. Excessive first pass metabolism, poor solubility and increased metabolism by CYP enzymes contribute to poor bioavailability of CBD and limit its clinical usage [47–49]

EVs derived from hUCMSCs have been explored as potential candidates to deliver anticancer agents [87, 88]. In this study, we isolated EVs from hUMSCs expanded by multilayer flasks and PBS-VW bioreactor followed by differential centrifugation using extra-PEG precipitation technique. We observed that there was no significant difference in particle size of EVs isolated from the above-mentioned methods. However, we observed 2.94-fold and 4.7-fold difference in the particle number and protein content when EVs were isolated from multilayer culture when compared to monolayer cultures, respectively. In addition, PBS-VW bioreactor was utilized to scale up the cell expansion and EVs production, which displayed a 2.48-fold increase in EVs protein content when compared to the EVs isolated from multilayer culture. Similarly, the zeta potential of the EVs isolated from bioreactor was comparable and relatively more stable without aggregation at storage temperatures (2–8°C) when compared to EVs isolated from monolayer and multilayer cultures. Generally, suspension culture in traditional bioreactors introduces potential stress to hMSCs which could damage cellular properties [115,116]. However, PBS-VW bioreactor potentially provide homogenous microenvironment to facilitate cell expansion while maintain low shear stress [117,118]. Thus, this microenvironment may also facilitate the production and cargo enrichment in the EVs. Although more studies are required to understand the effects of hydrodynamics on EVs biogenesis. Loading of drugs into EVs is a critical step and to date, multiple evidence demonstrates usage of incubation, sonication and electroporation techniques for loading of paclitaxel (PTX), curcumin, miRNAs and siRNAs inside the EVs [119]. In our study, initially we intended to compare the CBD loading and particle size difference in EVs after drug loading was carried out under both incubation and sonication methods. We optimized various parameters like buffer composition, pH, CBD loading, sonication cycles to get a superior optimized formulation. We observed that there was a 1.32-fold improvement in entrapment efficiency of CBD at 10 % loading using sonication in compared to incubation method. This may be due to enhanced permeabilization and interaction of lipophilic CBD with the EVs proteins. EVs loaded with CBD containing PBS, 0.1 % BSA and 10 % sucrose produced stable dispersion with a particle size of less than 130 nm and entrapment efficiency of more than 90 %. There was a slight decrease in particle size (10 nm) and entrapment efficiency (<5 %) upon storage for

1 month at refrigerated conditions (2–8°C). The CBD release from EVs was evaluated by dialysis method, where we observed a sustained release of CBD (i.e., >50 %) from the EVs at physiological buffer conditions, which mimics the environments of intestinal, extracellular matrix, blood and tumor cells. These observations corroborate well with earlier evidence, which demonstrates that paclitaxel loaded EVs have showed sustained release and superior anticancer effects *in vivo* [120].

In our study, we performed cytotoxicity assay of CBD and CBD EVs as well as the chemosensitization effect of CBD and CBD EVs in combination with DOX in 2D cultures of MDA-MB-231 cells. There was no significant difference between solution group as well as the EVs group, which is quite expected for *in-vitro* studies. Moreover, we observed there was a significant difference in G1 phase arrest when the MDA MB 231 WT cells were treated with CBD and CBD EVs as compared to control, suggesting that the cells are undergoing apoptosis.

Another important aspect of this research was to investigate the effect of same treatments in MDA-MB-231 Xenograft model of TNBC. Blank EVs have not shown any significant reduction in tumor volume as compared to control group. We assume that EVs were acting as delivery carriers for enhancing the effects of CBD to reduce the tumor burden in TNBC xenograft model. It was observed that CBD EVs + DOX combination significantly reduced the tumor burden when compared to control group, indicating better efficacy and promising clinical potential of CBD EVs + DOX. MDA-MB-231 cells treated with dye loaded EVs in 2D cultures have shown rapid increase in green fluorescence intensity. This suggests that the EVs could facilitate rapid internalization of cargo to the tumor cells possibly by endocytosis. Fluorescent EVs uptake study in MDA-MB-231 tumor tissue revealed presence of more EVs as observed by confocal microscopy. All these observations might be the reason for improved therapeutic efficacy of CBD when administered in EVs in our animal studies.

Inflammation plays a vital role in the development and progression of tumors [121]. Non-specific or specific inhibition of inflammatory mediators decrease the incidence and development of various cancers and thereby improved survivability [122,123]. Targeting inflammation is considered as a good approach for the therapy of various cancers [124]. Accumulating evidence suggests the anti-inflammatory potential of CBD in experimental models of various diseases [125–129]. We observed that CBD EVs (1 μM) or in combination of CBD EVs (1 μM) + DOX (500 nM) significantly decreased the expression of IL-17, STAT3 and p-STAT3, NF-κB proteins in MDA-MB-231 cells. Interestingly, we also observed decreased protein expression of IL-17, NF-κB and IL-6, TGF-β and NF-κB in tumor protein lysate of MDA-MB-231 cells when treated alone by CBD EVs (5 mg/kg) or in combination of CBD-EVs (5 mg/kg) and DOX (2 mg/kg) respectively.

Multiple evidence demonstrates that CBD inhibits the migration and invasion of various cancer cells [30,35,130,131]. We also investigated the effect of CBD EVs either alone or in combination with DOX on the migration of MDA-MB-231 cells by checking the expression of ITGA5, GPC1, GPC6, Smad-2 and Twist proteins. To date there are no reports showing the effect of CBD EVs either alone or in combination with DOX on GPC-1,−6, and ITGA5 in MDA-MB-231 cells. Smad-2 promotes the migration and invasion of various cancer

cells [132–134]. GPC1 regulates the proliferation, invasion and metastasis of tumor cells [135,136]. GPC6 is well demonstrated to promote the migration, invasion and proliferation of nasopharyngeal carcinoma [137]. Integrins decide the fate of cancer cells (i.e., whether to proliferate, die, migrate, or invade) in response to external stimuli [138,139]. Integrins play a vital role in the initiation and progression of breast cancer and regulation of stem cells biology [104,140]. Integrins are considered as novel therapeutic molecular targets in various cancer models [141,142]. ITGA5 regulates the adhesion, survival, and ECM component (i.e., fibronectin) mediated migration of breast cancer cells [143–145]. ITGA5 is also associated with lung and bone metastasis in models of breast cancer [146–148]. In our study, western blot analysis data of tumor protein lysate revealed that CBD-EVs (5 mg/kg) and DOX (2 mg/kg) significantly reduced the expression of ITGA5 compared to Control, DOX (2 mg/kg) and CBD (5 mg/kg) + DOX (2 mg/kg) group. This was further confirmed by immunocytochemistry staining in 2D cultures of MDA-MB-231 cells. Twist mediates the metastasis and epithelial-mesenchymal transition of breast cancer cells [149–151]. It was observed that CBD EVs and DOX combination significantly decreased the expression of Smad-2, GPC1, GPC6, ITGA5 and Twist proteins. Further we also assessed the effect of CBD EVs and DOX combination on the migration of MDA-MB-231 cells by using label-free real-time cell analysis platform (xCELLigence), which monitors the migration of cells through noninvasive electrical impedance. It was observed that CBD EVs and DOX combination significantly decreased the migration of MDA-MB-231 cells. All these results demonstrate the efficacy of CBD EVs either alone or in combination with DOX in inhibiting the migration and invasion of cancer cells.

Apoptosis (i.e., programmed cell death) is characterized by a series of cellular events which finally lead to the activation of cysteine proteases called caspases. Cancer cells adopt several strategies to evade apoptosis [152]. Dysregulation of apoptosis contributes to the development of cancer and chemotherapeutic drug resistance [153]. Determination of apoptotic processes disclose insights about the disease pathogenesis and the probable therapeutic options of how the disease can be effectively treated [154]. BAX, Bcl2 and BAX/Bcl2 ratio serve as prognostic markers in various cancers [155–157]. BAX/Bcl2 ratio and Caspase-8 and 9 are involved in the resistance of breast cancer cells to paclitaxel [158]. It was observed that CBD EVs (1 μM) + DOX (500 nM) combination significantly increased the expression of BAX and decreased the expression of Bcl2 in 2d cultures of MDA-MB-231 cells, when compared to other treatment groups. These findings were further evaluated by using tumor protein lysate from MDA-MB-231 cells after drug treatment. It was observed that CBD-EVs (5 mg/kg) and DOX (2 mg/kg) significantly decreased the expression of Bcl2, m-TOR and increased the expression of BAX and Caspase 9 when compared to other treatment groups.

5.2 Conclusion:

CBD EVs formulation was successfully formulated with desired average particle size, good entrapment efficiency and zeta potential by sonication method using EVs derived from hUCMSCs. CBD EVs by itself or in combination with DOX decreased the inflammation, metastasis and facilitated apoptosis in MDA-MB-231 cells by G1 phase cell cycle arrest and down regulation of IL-17, NF-κB, Twist, p-STAT3/STAT3 proteins *in-vitro*. Further, *in vivo* studies demonstrated that CBD EVs and DOX combination significantly reduced the tumor

burden (P<0.001) at a dose of 5mg/kg of CBD (5mg/kg) which was superior to 10mg/kg of free CBD. Further this combination modulated TME by decreasing the expression of TGF-β, IL-6, NF-κB, ITGA5, Smad-2, GPC 1&6, Twist and mediated apoptosis by increasing the expression of BAX, Caspase 9 and decreasing the expression of Bcl2. Our studies suggested that CBD EVs increased the sensitivity of MDA-MB-231tumor cells to DOX, thereby reducing the required effective dose of DOX thus abating or eliminating toxicity. Thus, EVs can be used as potential delivery systems for cannabinoids because of their easy internalization by tumors.

Supplementary Material

Refer to Web version on PubMed Central for supplementary material.

Acknowledgements

Authors are thankful to the Consortium for Medical Marijuana Clinical Outcomes Research, Grant/Award number: SUB00002097, National Institute on Minority Health and Health Disparities of National Institutes of Health, Grant/Award Number: U54 MD007582 and NSF-CREST Center for Complex Materials Design for Multidimensional Additive Processing (CoManD), Grant/Award Number:1735968 for providing the funding for this research work.

Data availability statement

The data that support the findings of our study are available from the corresponding author upon reasonable request.

Abbreviations:

EVs	Extracellular Vesicles
TNBC	triple negative breast cancer
CBD	cannabidiol
DOX	doxorubicin
DDS	drug delivery system
hUCMSCs	human Umbilical Cord Mesenchymal Stem Cells
NTA	nanoparticle tracking analysis
%EE	The percentage entrapment efficiency

References:

1. McKinney SM et al. Addendum: International evaluation of an AI system for breast cancer screening. Nature 586, E19, doi:10.1038/s41586-020-2679-9 (2020). [PubMed: 33057216]
2. Sun YS et al. Risk Factors and Preventions of Breast Cancer. Int J Biol Sci 13, 1387–1397, doi:10.7150/ijbs.21635 (2017). [PubMed: 29209143]
3. Ma JH, Qin L & Li X Role of STAT3 signaling pathway in breast cancer. Cell Commun Signal 18, 33, doi:10.1186/s12964-020-0527-z (2020). [PubMed: 32111215]

4. Surapaneni SK, Bhat ZR & Tikoo K MicroRNA-941 regulates the proliferation of breast cancer cells by altering histone H3 Ser 10 phosphorylation. Sci Rep 10, 17954, doi:10.1038/s41598-020-74847-7 (2020). [PubMed: 33087811]
5. Surapaneni SK, Bashir S & Tikoo K Gold nanoparticles-induced cytotoxicity in triple negative breast cancer involves different epigenetic alterations depending upon the surface charge. Sci Rep 8, 12295, doi:10.1038/s41598-018-30541-3 (2018). [PubMed: 30115982]
6. Yin L, Duan JJ, Bian XW & Yu SC Triple-negative breast cancer molecular subtyping and treatment progress. Breast Cancer Res 22, 61, doi:10.1186/s13058-020-01296-5 (2020). [PubMed: 32517735]
7. Hedrick E, Lee S-O, Doddapaneni R, Singh M & Safe S NR4A1 antagonists inhibit β1-integrin-dependent breast cancer cell migration. Molecular and cellular biology 36, 1383–1394 (2016). [PubMed: 26929200]
8. Patel K et al. Piperlongumine for enhancing oral bioavailability and cytotoxicity of docetaxel in triple-negative breast cancer. Journal of pharmaceutical sciences 104, 4417–4426 (2015). [PubMed: 26372815]
9. Pan YZ et al. Autophagy in drug resistance of the multiple myeloma cell line RPMI8226 to doxorubicin. Genet Mol Res 14, 5621–5629, doi:10.4238/2015.May.25.14 (2015). [PubMed: 26125760]
10. Tan Q et al. Src/STAT3-dependent heme oxygenase-1 induction mediates chemoresistance of breast cancer cells to doxorubicin by promoting autophagy. Cancer Sci 106, 1023–1032, doi:10.1111/cas.12712 (2015). [PubMed: 26041409]
11. Zhao L & Zhang B Doxorubicin induces cardiotoxicity through upregulation of death receptors mediated apoptosis in cardiomyocytes. Scientific reports 7, 1–11 (2017). [PubMed: 28127051]
12. Ghanem A et al. Tanshinone IIA synergistically enhances the antitumor activity of doxorubicin by interfering with the PI3K/AKT/mTOR pathway and inhibition of topoisomerase II: in vitro and molecular docking studies. New Journal of Chemistry 44, 17374–17381 (2020).
13. Andey T et al. Lipid nanocarriers of a lipid-conjugated estrogenic derivative inhibit tumor growth and enhance cisplatin activity against triple-negative breast cancer: pharmacokinetic and efficacy evaluation. Mol Pharm 12, 1105–1120, doi:10.1021/mp5008629 (2015). [PubMed: 25661724]
14. Griffin T et al. Potentiation of antitumor immunotoxins by liposomal monensin. J Natl Cancer Inst 85, 292–298, doi:10.1093/jnci/85.4.292 (1993). [PubMed: 8426373]
15. Singh M, Ghose T, Faulkner G, Kralovec J & Mezei M Targeting of methotrexate-containing liposomes with a monoclonal antibody against human renal cancer. Cancer Res 49, 3976–3984 (1989). [PubMed: 2660984]
16. Arthur P et al. Targeting lung cancer stem cells using combination of Tel and Docetaxel liposomes in 3D cultures and tumor xenografts. Toxicol Appl Pharmacol 401, 115112, doi:10.1016/j.taap.2020.115112 (2020). [PubMed: 32540278]
17. Li RJ et al. All-trans retinoic acid stealth liposomes prevent the relapse of breast cancer arising from the cancer stem cells. J Control Release 149, 281–291, doi:10.1016/j.jconrel.2010.10.019 (2011). [PubMed: 20971141]
18. Gulati M, Grover M, Singh M & Singh S Study of azathioprine encapsulation into liposomes. J Microencapsul 15, 485–494, doi:10.3109/02652049809006875 (1998). [PubMed: 9651870]
19. Ferdous AJ, Stembridge NY & Singh M Role of monensin PLGA polymer nanoparticles and liposomes as potentiator of ricin A immunotoxins in vitro. Journal of controlled release 50, 71–78 (1998). [PubMed: 9685874]
20. Gulati M, Grover M, Singh M & Singh S Study of azathioprine encapsulation into liposomes. Journal of microencapsulation 15, 485–494 (1998). [PubMed: 9651870]
21. Andey T et al. Lipid nanocarriers of a lipid-conjugated estrogenic derivative inhibit tumor growth and enhance cisplatin activity against triple-negative breast cancer: pharmacokinetic and efficacy evaluation. Molecular pharmaceutics 12, 1105–1120 (2015). [PubMed: 25661724]
22. Singh M, Ghose T, Faulkner G, Kralovec J & Mezei M Targeting of methotrexate-containing liposomes with a monoclonal antibody against human renal cancer. Cancer research 49, 3976–3984 (1989). [PubMed: 2660984]
23. Griffin T et al. Potentiation of antitumor immunotoxins by liposomal monensin. JNCI: Journal of the National Cancer Institute 85, 292–298 (1993). [PubMed: 8426373]

24. Boakye CH, Patel K & Singh M Doxorubicin liposomes as an investigative model to study the skin permeation of nanocarriers. International journal of pharmaceutics 489, 106–116 (2015). [PubMed: 25910414]
25. Doddapaneni R, Patel K, Owaid IH & Singh M Tumor neovasculature-targeted cationic PEGylated liposomes of gambogic acid for the treatment of triple-negative breast cancer. Drug delivery 23, 1232–1241 (2016). [PubMed: 26701717]
26. Gu X et al. Nano-delivery systems focused on tumor microenvironment regulation and biomimetic strategies for treatment of breast cancer metastasis. J Control Release 333, 374–390, doi:10.1016/j.jconrel.2021.03.039 (2021). [PubMed: 33798666]
27. Guzmán M Cannabinoids: potential anticancer agents. Nat Rev Cancer 3, 745–755, doi:10.1038/nrc1188 (2003). [PubMed: 14570037]
28. Sarfaraz S, Adhami VM, Syed DN, Afaq F & Mukhtar H Cannabinoids for cancer treatment: progress and promise. Cancer Res 68, 339–342, doi:10.1158/0008-5472.Can-07-2785 (2008). [PubMed: 18199524]
29. Alexander A, Smith PF & Rosengren RJ Cannabinoids in the treatment of cancer. Cancer letters 285, 6–12 (2009). [PubMed: 19442435]
30. McAllister SD et al. Pathways mediating the effects of cannabidiol on the reduction of breast cancer cell proliferation, invasion, and metastasis. Breast Cancer Res Treat 129, 37–47, doi:10.1007/s10549-010-1177-4 (2011). [PubMed: 20859676]
31. Tomko AM, Whynot EG, Ellis LD & Dupré DJ Anti-Cancer Potential of Cannabinoids, Terpenes, and Flavonoids Present in Cannabis. Cancers (Basel) 12, doi:10.3390/cancers12071985 (2020).
32. Greish K et al. Synthetic cannabinoids nano-micelles for the management of triple negative breast cancer. J Control Release 291, 184–195, doi:10.1016/j.jconrel.2018.10.030 (2018). [PubMed: 30367922]
33. Kenyon J, Liu W & Dalgleish A Report of Objective Clinical Responses of Cancer Patients to Pharmaceutical-grade Synthetic Cannabidiol. Anticancer Res 38, 5831–5835, doi:10.21873/anticanres.12924 (2018). [PubMed: 30275207]
34. Sultan AS, Marie MA & Sheweita SA Novel mechanism of cannabidiol-induced apoptosis in breast cancer cell lines. Breast 41, 34–41, doi:10.1016/j.breast.2018.06.009 (2018). [PubMed: 30007266]
35. Elbaz M et al. Modulation of the tumor microenvironment and inhibition of EGF/EGFR pathway: novel anti-tumor mechanisms of Cannabidiol in breast cancer. Mol Oncol 9, 906–919, doi:10.1016/j.molonc.2014.12.010 (2015). [PubMed: 25660577]
36. McAllister SD, Christian RT, Horowitz MP, Garcia A & Desprez PY Cannabidiol as a novel inhibitor of Id-1 gene expression in aggressive breast cancer cells. Mol Cancer Ther 6, 2921–2927, doi:10.1158/1535-7163.Mct-07-0371 (2007). [PubMed: 18025276]
37. Hernán Pérez de la Ossa D et al. Poly-ɛ-caprolactone microspheres as a drug delivery system for cannabinoid administration: development, characterization and in vitro evaluation of their antitumoral efficacy. J Control Release 161, 927–932, doi:10.1016/j.jconrel.2012.05.003 (2012). [PubMed: 22580111]
38. García-Morales L et al. CBD Reverts the Mesenchymal Invasive Phenotype of Breast Cancer Cells Induced by the Inflammatory Cytokine IL-1β. Int J Mol Sci 21, doi:10.3390/ijms21072429 (2020).
39. Preet A et al. Cannabinoid receptors, CB1 and CB2, as novel targets for inhibition of non-small cell lung cancer growth and metastasis. Cancer Prev Res (Phila) 4, 65–75, doi:10.1158/1940-6207.Capr-10-0181 (2011). [PubMed: 21097714]
40. Massi P, Solinas M, Cinquina V & Parolaro D Cannabidiol as potential anticancer drug. Br J Clin Pharmacol 75, 303–312, doi:10.1111/j.1365-2125.2012.04298.x (2013). [PubMed: 22506672]
41. Sreevalsan S, Joseph S, Jutooru I, Chadalapaka G & Safe SH Induction of apoptosis by cannabinoids in prostate and colon cancer cells is phosphatase dependent. Anticancer Res 31, 3799–3807 (2011). [PubMed: 22110202]
42. Velasco G, Sánchez C & Guzmán M Towards the use of cannabinoids as antitumour agents. Nat Rev Cancer 12, 436–444, doi:10.1038/nrc3247 (2012). [PubMed: 22555283]
43. Torres S et al. A combined preclinical therapy of cannabinoids and temozolomide against glioma. Molecular cancer therapeutics 10, 90–103 (2011). [PubMed: 21220494]

44. Scott KA, Dalgleish AG & Liu WM The combination of cannabidiol and Δ9-tetrahydrocannabinol enhances the anticancer effects of radiation in an orthotopic murine glioma model. Molecular cancer therapeutics 13, 2955–2967 (2014). [PubMed: 25398831]
45. Fraguas-Sánchez AI et al. Enhancing ovarian cancer conventional chemotherapy through the combination with cannabidiol loaded microparticles. Eur J Pharm Biopharm 154, 246–258, doi:10.1016/j.ejpb.2020.07.008 (2020). [PubMed: 32682943]
46. Nabissi M, Morelli MB, Santoni M & Santoni G Triggering of the TRPV2 channel by cannabidiol sensitizes glioblastoma cells to cytotoxic chemotherapeutic agents. Carcinogenesis 34, 48–57, doi:10.1093/carcin/bgs328 (2013). [PubMed: 23079154]
47. Hunt CA, Jones RT, Herning RI & Bachman J Evidence that cannabidiol does not significantly alter the pharmacokinetics of tetrahydrocannabinol in man. Journal of pharmacokinetics and biopharmaceutics 9, 245–260 (1981). [PubMed: 6270295]
48. Watanabe K, Yamaori S, Funahashi T, Kimura T & Yamamoto I Cytochrome P450 enzymes involved in the metabolism of tetrahydrocannabinols and cannabinol by human hepatic microsomes. Life Sci 80, 1415–1419, doi:10.1016/j.lfs.2006.12.032 (2007). [PubMed: 17303175]
49. Zendulka O et al. Cannabinoids and Cytochrome P450 Interactions. Curr Drug Metab 17, 206–226, doi:10.2174/1389200217666151210142051 (2016). [PubMed: 26651971]
50. Bruni N et al. Cannabinoid delivery systems for pain and inflammation treatment. Molecules 23, 2478 (2018).
51. Mannila J, Järvinen T, Järvinen K & Jarho P Precipitation complexation method produces cannabidiol/β-cyclodextrin inclusion complex suitable for sublingual administration of cannabidiol. Journal of pharmaceutical sciences 96, 312–319 (2007). [PubMed: 17051591]
52. Mojsa AV (Google Patents, 2019).
53. Szaflarski JP et al. Higher cannabidiol plasma levels are associated with better seizure response following treatment with a pharmaceutical grade cannabidiol. Epilepsy & Behavior 95, 131–136 (2019). [PubMed: 31048098]
54. Millar SA, Stone NL, Yates AS & O'Sullivan SE A systematic review on the pharmacokinetics of cannabidiol in humans. Frontiers in pharmacology 9, 1365 (2018). [PubMed: 30534073]
55. Zenone M, Snyder J & Caulfield T Crowdfunding Cannabidiol (CBD) for Cancer: Hype and Misinformation on GoFundMe. Am J Public Health 110, S294–s299, doi:10.2105/ajph.2020.305768 (2020). [PubMed: 33001729]
56. Fraguas-Sánchez AI et al. PLGA Nanoparticles for the Intraperitoneal Administration of CBD in the Treatment of Ovarian Cancer: In Vitro and In Ovo Assessment. Pharmaceutics 12, doi:10.3390/pharmaceutics12050439 (2020).
57. Fraguas-Sánchez AI, Fernández-Carballido A, Simancas-Herbada R, Martin-Sabroso C & Torres-Suárez AI CBD loaded microparticles as a potential formulation to improve paclitaxel and doxorubicin-based chemotherapy in breast cancer. Int J Pharm 574, 118916, doi:10.1016/j.ijpharm.2019.118916 (2020). [PubMed: 31811927]
58. Brinton LT, Sloane HS, Kester M & Kelly KA Formation and role of exosomes in cancer. Cellular and molecular life sciences 72, 659–671 (2015). [PubMed: 25336151]
59. Fais S et al. Exosomes: the ideal nanovectors for biodelivery. Biological chemistry 394, 1–15, doi:10.1515/hsz-2012-0236 (2013). [PubMed: 23241589]
60. Zhang M et al. Exosome-based nanocarriers as bio-inspired and versatile vehicles for drug delivery: recent advances and challenges. Journal of Materials Chemistry B 7, 2421–2433 (2019). [PubMed: 32255119]
61. Kwon S et al. Engineering approaches for effective therapeutic applications based on extracellular vesicles. J Control Release 330, 15–30, doi:10.1016/j.jconrel.2020.11.062 (2021). [PubMed: 33278480]
62. Kooijmans SA, Vader P, van Dommelen SM, van Solinge WW & Schiffelers RM Exosome mimetics: a novel class of drug delivery systems. International journal of nanomedicine 7, 1525 (2012). [PubMed: 22619510]
63. Kalluri R The biology and function of exosomes in cancer. The Journal of clinical investigation 126, 1208–1215 (2016). [PubMed: 27035812]

64. Osaki M & Okada F Exosomes and Their Role in Cancer Progression. Yonago Acta Medica 62, 182–190 (2019). [PubMed: 31320822]
65. Wee I, Syn N, Sethi G, Goh BC & Wang L Role of tumor-derived exosomes in cancer metastasis. Biochimica et Biophysica Acta (BBA)-Reviews on Cancer (2018).
66. Zhang C, Ji Q, Yang Y, Li Q & Wang Z Exosome: Function and role in cancer metastasis and drug resistance. Technology in cancer research & treatment 17, 1533033818763450 (2018). [PubMed: 29681222]
67. Whiteside TL in Advances in clinical chemistry Vol. 74 103–141 (Elsevier, 2016). [PubMed: 27117662]
68. Tai YL, Chen KC, Hsieh JT & Shen TL Exosomes in cancer development and clinical applications. Cancer science 109, 2364–2374 (2018). [PubMed: 29908100]
69. Zhang X et al. Exosomes in cancer: small particle, big player. Journal of hematology & oncology 8, 83 (2015). [PubMed: 26156517]
70. Elahi FM, Farwell DG, Nolta JA & Anderson JD Concise Review: Preclinical Translation of Exosomes Derived from Mesenchymal Stem/Stromal Cells. STEM CELLS (2019).
71. Crivelli B et al. Mesenchymal stem/stromal cell extracellular vesicles: From active principle to next generation drug delivery system. J Control Release 262, 104–117, doi:10.1016/j.jconrel.2017.07.023 (2017). [PubMed: 28736264]
72. Yin K, Wang S & Zhao RC Exosomes from mesenchymal stem/stromal cells: a new therapeutic paradigm. Biomarker research 7, 8 (2019). [PubMed: 30992990]
73. Lee J-K et al. Exosomes derived from mesenchymal stem cells suppress angiogenesis by down-regulating VEGF expression in breast cancer cells. PloS one 8, e84256 (2013). [PubMed: 24391924]
74. Ma J et al. Exosomes derived from AKt-modified human umbilical cord mesenchymal stem cells improve cardiac regeneration and promote angiogenesis via activating platelet-derived growth factor D. Stem cells translational medicine 6, 51–59 (2017). [PubMed: 28170176]
75. Li T et al. Exosomes derived from human umbilical cord mesenchymal stem cells alleviate liver fibrosis. Stem cells and development 22, 845–854 (2013). [PubMed: 23002959]
76. Goodarzi P et al. in Cell Biology and Translational Medicine, Volume 4 119–131 (Springer, 2018).
77. Rani S, Ryan AE, Griffin MD & Ritter T Mesenchymal stem cell-derived extracellular vesicles: toward cell-free therapeutic applications. Molecular Therapy 23, 812–823 (2015). [PubMed: 25868399]
78. Kommineni N, Meckes D & Sachdeva M Exosome Vehicles as Nano-Drug Delivery Materials for Chemotherapeutic Drugs. Critical Reviews™ in Therapeutic Drug Carrier Systems.
79. Cheng L, Zhang K, Wu S, Cui M & Xu T Focus on mesenchymal stem cell-derived exosomes: opportunities and challenges in cell-free therapy. Stem cells international 2017 (2017).
80. Dong R et al. MSC-Derived Exosomes-Based Therapy for Peripheral Nerve Injury: A Novel Therapeutic Strategy. BioMed research international 2019 (2019).
81. Shiue SJ et al. Mesenchymal stem cell exosomes as a cell-free therapy for nerve injury-induced pain in rats. Pain 160, 210–223, doi:10.1097/j.pain.0000000000001395 (2019). [PubMed: 30188455]
82. Yuan X, Tsai AC, Farrance I, Rowley J & Ma T Aggregation of Culture Expanded Human Mesenchymal Stem Cells in Microcarrier-based Bioreactor. Biochem Eng J 131, 39–46, doi:10.1016/j.bej.2017.12.011 (2018). [PubMed: 29736144]
83. Tsai AC, Jeske R, Chen X, Yuan X & Li Y Influence of Microenvironment on Mesenchymal Stem Cell Therapeutic Potency: From Planar Culture to Microcarriers. Front Bioeng Biotechnol 8, 640, doi:10.3389/fbioe.2020.00640 (2020). [PubMed: 32671039]
84. Hedrick E, Lee SO, Doddapaneni R, Singh M & Safe S Nuclear receptor 4A1 as a drug target for breast cancer chemotherapy. Endocr Relat Cancer 22, 831–840, doi:10.1530/erc-15-0063 (2015). [PubMed: 26229035]
85. Saingam W & Sakunpak A Development and validation of reverse phase high performance liquid chromatography method for the determination of delta-9-tetrahydrocannabinol and cannabidiol in oromucosal spray from cannabis extract. Revista Brasileira de Farmacognosia 28, 669–672 (2018).

86. Hurwitz SN et al. CD63 regulates epstein-barr virus LMP1 exosomal packaging, enhancement of vesicle production, and noncanonical NF-κB signaling. Journal of virology 91 (2017).
87. Hurwitz SN & Meckes DG in Extracellular Vesicles 303–317 (Springer, 2017).
88. Hurwitz SN, Cheerathodi MR, Nkosi D, York SB & Meckes DG Tetraspanin CD63 bridges autophagic and endosomal processes to regulate exosomal secretion and intracellular signaling of Epstein-Barr virus LMP1. Journal of virology 92 (2018).
89. Rider MA, Hurwitz SN & Meckes DG Jr ExtraPEG: a polyethylene glycol-based method for enrichment of extracellular vesicles. Scientific reports 6, 23978 (2016). [PubMed: 27068479]
90. Lötvall J et al. (Wiley Online Library, 2014).
91. Witwer KW et al. (Wiley Online Library, 2017).
92. Mehdiani A et al. An innovative method for exosome quantification and size measurement. JoVE (Journal of Visualized Experiments), e50974 (2015).
93. Lässer C, Eldh M & Lötvall J Isolation and characterization of RNA-containing exosomes. JoVE (Journal of Visualized Experiments), e3037 (2012). [PubMed: 22257828]
94. Kommineni N et al. Role of nano-lipid formulation of CARP-1 mimetic, CFM-4.17 to improve systemic exposure and response in osimertinib resistant non-small cell lung cancer. Eur J Pharm Biopharm 158, 172–184, doi:10.1016/j.ejpb.2020.11.007 (2021). [PubMed: 33220423]
95. Kommineni N, Saka R, Bulbake U & Khan W Cabazitaxel and thymoquinone co-loaded lipospheres as a synergistic combination for breast cancer. Chemistry and physics of lipids 224, 104707 (2019). [PubMed: 30521787]
96. Kommineni N, Mahira S, Domb AJ & Khan W Cabazitaxel-loaded nanocarriers for cancer therapy with reduced side effects. Pharmaceutics 11, 141 (2019).
97. Kommineni N et al. Role of nano-lipid formulation of CARP-1 mimetic, CFM-4.17 to improve systemic exposure and response in osimertinib resistant non-small cell lung cancer. European Journal of Pharmaceutics and Biopharmaceutics 158, 172–184 (2021). [PubMed: 33220423]
98. Liu XF, Yang WT, Xu R, Liu JT & Zheng PS Cervical cancer cells with positive Sox2 expression exhibit the properties of cancer stem cells. PLoS One 9, e87092, doi:10.1371/journal.pone.0087092 (2014). [PubMed: 24489842]
99. Liu X et al. Expression of hiwi gene in human gastric cancer was associated with proliferation of cancer cells. Int J Cancer 118, 1922–1929, doi:10.1002/ijc.21575 (2006). [PubMed: 16287078]
100. Kalvala AK et al. Chronic hyperglycemia impairs mitochondrial unfolded protein response and precipitates proteotoxicity in experimental diabetic neuropathy: focus on LonP1 mediated mitochondrial regulation. Pharmacol Rep 72, 1627–1644, doi:10.1007/s43440-020-00147-6 (2020). [PubMed: 32720218]
101. Arthur P et al. Targeting lung cancer stem cells using combination of Tel and Docetaxel liposomes in 3D cultures and tumor xenografts. Toxicology and applied pharmacology 401, 115112 (2020). [PubMed: 32540278]
102. Salarpour S et al. Paclitaxel incorporated exosomes derived from glioblastoma cells: comparative study of two loading techniques. DARU Journal of Pharmaceutical Sciences 27, 533–539 (2019). [PubMed: 31317441]
103. Carcereri de Prati A et al. Metastatic Breast Cancer Cells Enter Into Dormant State and Express Cancer Stem Cells Phenotype Under Chronic Hypoxia. J Cell Biochem 118, 3237–3248, doi:10.1002/jcb.25972 (2017). [PubMed: 28262977]
104. Hedrick E, Lee SO, Doddapaneni R, Singh M & Safe S NR4A1 Antagonists Inhibit β1-Integrin-Dependent Breast Cancer Cell Migration. Mol Cell Biol 36, 1383–1394, doi:10.1128/mcb.00912-15 (2016). [PubMed: 26929200]
105. Hartman ZC et al. Growth of triple-negative breast cancer cells relies upon coordinate autocrine expression of the proinflammatory cytokines IL-6 and IL-8. Cancer Res 73, 3470–3480, doi:10.1158/0008-5472.Can-12-4524-t (2013). [PubMed: 23633491]
106. Asad S et al. Sociodemographic Factors Associated With Rapid Relapse in Triple-Negative Breast Cancer: A Multi-Institution Study. Journal of the National Comprehensive Cancer Network 1, 1–8 (2021).

107. Carty N, Foggitt A, Hamilton C, Royle G & Taylor I Patterns of clinical metastasis in breast cancer: an analysis of 100 patients. European Journal of Surgical Oncology (EJSO) 21, 607–608 (1995). [PubMed: 8631404]
108. Grobmyer SR et al. Nanoparticle delivery for metastatic breast cancer. Nanomedicine: Nanotechnology, Biology and Medicine 8, S21–S30 (2012).
109. Li Z et al. Dexamethasone induces docetaxel and cisplatin resistance partially through upregulating Krüppel-like factor 5 in triple-negative breast cancer. Oncotarget 8, 11555–11565, doi:10.18632/oncotarget.14135 (2017). [PubMed: 28030791]
110. Seligson JM, Patron AM, Berger MJ, Harvey RD & Seligson ND Sacituzumab Govitecan-hziy: An Antibody-Drug Conjugate for the Treatment of Refractory, Metastatic, Triple-Negative Breast Cancer. Annals of Pharmacotherapy, 1060028020966548 (2020).
111. Sultan AS, Marie MA & Sheweita SA Novel mechanism of cannabidiol-induced apoptosis in breast cancer cell lines. The Breast 41, 34–41 (2018). [PubMed: 30007266]
112. Williamson EM & Evans FJ Cannabinoids in clinical practice. Drugs 60, 1303–1314 (2000). [PubMed: 11152013]
113. Seltzer ES, Watters AK, MacKenzie D, Granat LM & Zhang D Cannabidiol (CBD) as a Promising Anti-Cancer Drug. Cancers 12, 3203 (2020).
114. Howlett AC & Shim J-Y in Madame Curie Bioscience Database [Internet] (Landes Bioscience, 2013).
115. Jeske R et al. Agitation in a microcarrier-based spinner flask bioreactor modulates homeostasis of human mesenchymal stem cells. Biochemical Engineering Journal 168, 107947 (2021). [PubMed: 33967591]
116. Wyrobnik TA, Ducci A & Micheletti M Advances in human mesenchymal stromal cell-based therapies - Towards an integrated biological and engineering approach. Stem Cell Res 47, 101888, doi:10.1016/j.scr.2020.101888 (2020). [PubMed: 32688331]
117. Nogueira DES et al. Strategies for the expansion of human induced pluripotent stem cells as aggregates in single-use Vertical-Wheel™ bioreactors. J Biol Eng 13, 74, doi:10.1186/s13036-019-0204-1 (2019). [PubMed: 31534477]
118. de Sousa Pinto D et al. Scalable Manufacturing of Human Mesenchymal Stromal Cells in the Vertical-Wheel Bioreactor System: An Experimental and Economic Approach. Biotechnol J 14, e1800716, doi:10.1002/biot.201800716 (2019). [PubMed: 30945467]
119. Wang J, Chen D & Ho EA Challenges in the development and establishment of exosome-based drug delivery systems. Journal of Controlled Release (2020).
120. Pascucci L et al. Paclitaxel is incorporated by mesenchymal stromal cells and released in exosomes that inhibit in vitro tumor growth: a new approach for drug delivery. Journal of Controlled Release 192, 262–270 (2014). [PubMed: 25084218]
121. Greten FR & Grivennikov SI Inflammation and Cancer: Triggers, Mechanisms, and Consequences. Immunity 51, 27–41, doi:10.1016/j.immuni.2019.06.025 (2019). [PubMed: 31315034]
122. Ridker PM et al. Effect of interleukin-1β inhibition with canakinumab on incident lung cancer in patients with atherosclerosis: exploratory results from a randomised, double-blind, placebo-controlled trial. Lancet 390, 1833–1842, doi:10.1016/s0140-6736(17)32247-x (2017). [PubMed: 28855077]
123. Rothwell PM et al. Effect of daily aspirin on risk of cancer metastasis: a study of incident cancers during randomised controlled trials. Lancet 379, 1591–1601, doi:10.1016/s0140-6736(12)60209-8 (2012). [PubMed: 22440947]
124. Ritter B & Greten FR Modulating inflammation for cancer therapy. J Exp Med 216, 1234–1243, doi:10.1084/jem.20181739 (2019). [PubMed: 31023715]
125. Hammell DC et al. Transdermal cannabidiol reduces inflammation and pain-related behaviours in a rat model of arthritis. Eur J Pain 20, 936–948, doi:10.1002/ejp.818 (2016). [PubMed: 26517407]
126. Vuolo F et al. Cannabidiol reduces airway inflammation and fibrosis in experimental allergic asthma. Eur J Pharmacol 843, 251–259, doi:10.1016/j.ejphar.2018.11.029 (2019). [PubMed: 30481497]

127. Sangiovanni E et al. Cannabis sativa L. extract and cannabidiol inhibit in vitro mediators of skin inflammation and wound injury. Phytother Res 33, 2083–2093, doi:10.1002/ptr.6400 (2019). [PubMed: 31250491]
128. Wang Y et al. Cannabidiol attenuates alcohol-induced liver steatosis, metabolic dysregulation, inflammation and neutrophil-mediated injury. Sci Rep 7, 12064, doi:10.1038/s41598-017-10924-8 (2017). [PubMed: 28935932]
129. Dos-Santos-Pereira M, Guimarães FS, Del-Bel E, Raisman-Vozari R & Michel PP Cannabidiol prevents LPS-induced microglial inflammation by inhibiting ROS/NF-κB-dependent signaling and glucose consumption. Glia 68, 561–573, doi:10.1002/glia.23738 (2020). [PubMed: 31647138]
130. Vaccani A, Massi P, Colombo A, Rubino T & Parolaro D Cannabidiol inhibits human glioma cell migration through a cannabinoid receptor-independent mechanism. Br J Pharmacol 144, 1032–1036, doi:10.1038/sj.bjp.0706134 (2005). [PubMed: 15700028]
131. Ramer R, Merkord J, Rohde H & Hinz B Cannabidiol inhibits cancer cell invasion via upregulation of tissue inhibitor of matrix metalloproteinases-1. Biochem Pharmacol 79, 955–966, doi:10.1016/j.bcp.2009.11.007 (2010). [PubMed: 19914218]
132. Lv ZD et al. Transforming growth factor-β 1 enhances the invasiveness of breast cancer cells by inducing a Smad2-dependent epithelial-to-mesenchymal transition. Oncol Rep 29, 219–225, doi:10.3892/or.2012.2111 (2013). [PubMed: 23129177]
133. Cao WH et al. USP4 promotes invasion of breast cancer cells via Relaxin/TGF-β1/Smad2/MMP-9 signal. Eur Rev Med Pharmacol Sci 20, 1115–1122 (2016). [PubMed: 27049265]
134. Kumar KJ, Vani MG, Chueh PJ, Mau JL & Wang SY Antrodin C inhibits epithelial-to-mesenchymal transition and metastasis of breast cancer cells via suppression of Smad2/3 and β-catenin signaling pathways. PLoS One 10, e0117111, doi:10.1371/journal.pone.0117111 (2015). [PubMed: 25658913]
135. Matsuda K et al. Glypican-1 is overexpressed in human breast cancer and modulates the mitogenic effects of multiple heparin-binding growth factors in breast cancer cells. Cancer Res 61, 5562–5569 (2001). [PubMed: 11454708]
136. Lund ME, Campbell DH & Walsh BJ The Role of Glypican-1 in the Tumour Microenvironment. Adv Exp Med Biol 1245, 163–176, doi:10.1007/978-3-030-40146-7_8 (2020). [PubMed: 32266658]
137. Fan C et al. GPC6 Promotes Cell Proliferation, Migration, and Invasion in Nasopharyngeal Carcinoma. J Cancer 10, 3926–3932, doi:10.7150/jca.31345 (2019). [PubMed: 31417636]
138. Guo W & Giancotti FG Integrin signalling during tumour progression. Nat Rev Mol Cell Biol 5, 816–826, doi:10.1038/nrm1490 (2004). [PubMed: 15459662]
139. Stupack DG Integrins as a distinct subtype of dependence receptors. Cell Death Differ 12, 1021–1030, doi:10.1038/sj.cdd.4401658 (2005). [PubMed: 15933741]
140. Pontier SM & Muller WJ Integrins in mammary-stem-cell biology and breast-cancer progression--a role in cancer stem cells? J Cell Sci 122, 207–214, doi:10.1242/jcs.040394 (2009). [PubMed: 19118213]
141. Aksorn N & Chanvorachote P Integrin as a Molecular Target for Anti-cancer Approaches in Lung Cancer. Anticancer Res 39, 541–548, doi:10.21873/anticanres.13146 (2019). [PubMed: 30711928]
142. Tucker GC Integrins: molecular targets in cancer therapy. Curr Oncol Rep 8, 96–103, doi:10.1007/s11912-006-0043-3 (2006). [PubMed: 16507218]
143. Qin L et al. Steroid receptor coactivator-1 upregulates integrin α_5 expression to promote breast cancer cell adhesion and migration. Cancer Res 71, 1742–1751, doi:10.1158/0008-5472.Can-10-3453 (2011). [PubMed: 21343398]
144. Korah R, Boots M & Wieder R Integrin alpha5beta1 promotes survival of growth-arrested breast cancer cells: an in vitro paradigm for breast cancer dormancy in bone marrow. Cancer Res 64, 4514–4522, doi:10.1158/0008-5472.Can-03-3853 (2004). [PubMed: 15231661]
145. Van der Velde-Zimmermann D et al. Fibronectin distribution in human bone marrow stroma: matrix assembly and tumor cell adhesion via alpha5 beta1 integrin. Exp Cell Res 230, 111–120, doi:10.1006/excr.1996.3405 (1997). [PubMed: 9013713]

146. Yao H, Veine DM & Livant DL Therapeutic inhibition of breast cancer bone metastasis progression and lung colonization: breaking the vicious cycle by targeting α5β1 integrin. Breast Cancer Res Treat 157, 489–501, doi:10.1007/s10549-016-3844-6 (2016). [PubMed: 27255534]

147. Ju JA et al. Hypoxia Selectively Enhances Integrin α(5)β(1) Receptor Expression in Breast Cancer to Promote Metastasis. Mol Cancer Res 15, 723–734, doi:10.1158/1541-7786.Mcr-16-0338 (2017). [PubMed: 28213554]

148. Pantano F et al. Integrin alpha5 in human breast cancer is a mediator of bone metastasis and a therapeutic target for the treatment of osteolytic lesions. Oncogene, doi:10.1038/s41388-020-01603-6 (2021).

149. Kim MS et al. MEST induces Twist-1-mediated EMT through STAT3 activation in breast cancers. Cell Death Differ 26, 2594–2606, doi:10.1038/s41418-019-0322-9 (2019). [PubMed: 30903102]

150. Cao J et al. Twist promotes tumor metastasis in basal-like breast cancer by transcriptionally upregulating ROR1. Theranostics 8, 2739–2751, doi:10.7150/thno.21477 (2018). [PubMed: 29774072]

151. Zhang D. r., Wang W. l., WU L-X & Liu M.-r. Twist promotes cell migration and invasion in human breast cancer cell line Hs578T. Basic & Clinical Medicine 38, 771 (2018).

152. Fernald K & Kurokawa M Evading apoptosis in cancer. Trends in cell biology 23, 620–633 (2013). [PubMed: 23958396]

153. Brown JM & Attardi LD The role of apoptosis in cancer development and treatment response. Nat Rev Cancer 5, 231–237, doi:10.1038/nrc1560 (2005). [PubMed: 15738985]

154. Wong RS Apoptosis in cancer: from pathogenesis to treatment. J Exp Clin Cancer Res 30, 87, doi:10.1186/1756-9966-30-87 (2011). [PubMed: 21943236]

155. Kulsoom B et al. Bax, Bcl-2, and Bax/Bcl-2 as prognostic markers in acute myeloid leukemia: are we ready for Bcl-2-directed therapy? Cancer Manag Res 10, 403–416, doi:10.2147/cmar.S154608 (2018). [PubMed: 29535553]

156. Matsumoto H et al. Bax to Bcl-2 ratio and Ki-67 index are useful predictors of neoadjuvant chemoradiation therapy in bladder cancer. Jpn J Clin Oncol 34, 124–130, doi:10.1093/jjco/hyh026 (2004). [PubMed: 15078907]

157. Khodapasand E, Jafarzadeh N, Farrokhi F, Kamalidehghan B & Houshmand M Is Bax/Bcl-2 ratio considered as a prognostic marker with age and tumor location in colorectal cancer? Iran Biomed J 19, 69–75, doi:10.6091/ibj.1366.2015 (2015). [PubMed: 25864810]

158. Sharifi S, Barar J, Hejazi MS & Samadi N Roles of the Bcl-2/Bax ratio, caspase-8 and 9 in resistance of breast cancer cells to paclitaxel. Asian Pac J Cancer Prev 15, 8617–8622, doi:10.7314/apjcp.2014.15.20.8617 (2014). [PubMed: 25374178]

Highlights

- CBD loaded extracellular vesicles (CBD EVs) were successfully formulated for the first time with good entrapment efficiency and particle size
- Sustained release of CBD was observed from CBD EVs
- Fluorescent labelled EVs showed rapid intracellular and intratumoral uptake as determined by confocal microscopy
- CBD EVs (5 mg/kg) and doxorubicin (DOX) combination significantly reduced the tumor burden in MDA-MB-231 xenograft model of athymic nude mice
- CBD EVs sensitized the MDA-MB-231 tumors to DOX by decreasing inflammation, migration, metastasis and facilitating apoptosis

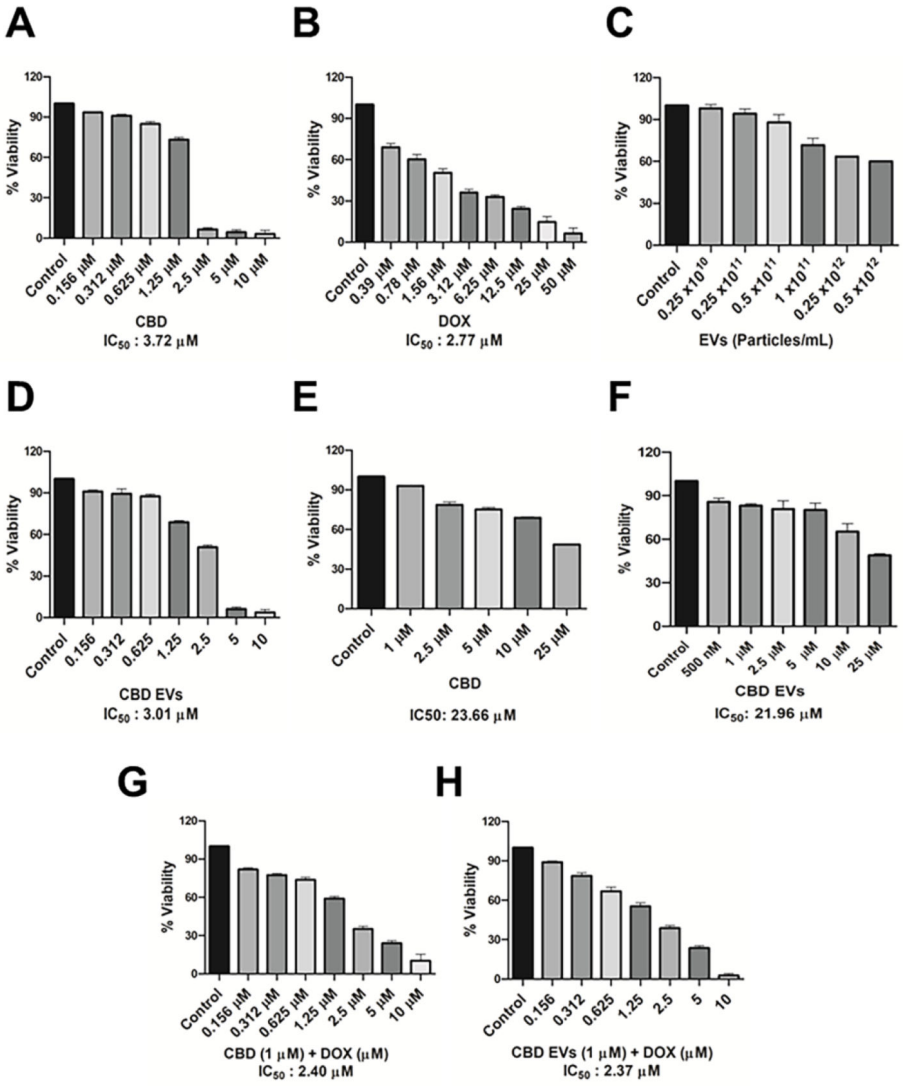

Figure 1:

hUCMSCs cultured on Cytodex-1 microcarriers in PBS-VW bioreactor. A. Hoechst staining of hUCMSCs on microcarrier in PBS-VW bioreactor on Day 1, 3, 5 and 8. B. Glucose and lactate concentration for hUCMSCs in PBS-VW bioreactor. C. Weight ratio of glucose consumption over lactate production in the bioreactor system. D. Mean particle size distribution graph for CBD loaded EVs by sonication method. E. TEM image of EVs. F. Fluorescently labelled EVs uptake in MDA MB 231 cells. G. *In-vitro* CBD release from EVs in PBS at pH- 6.8 and 7.4 representing % cumulative CBD released Vs time.

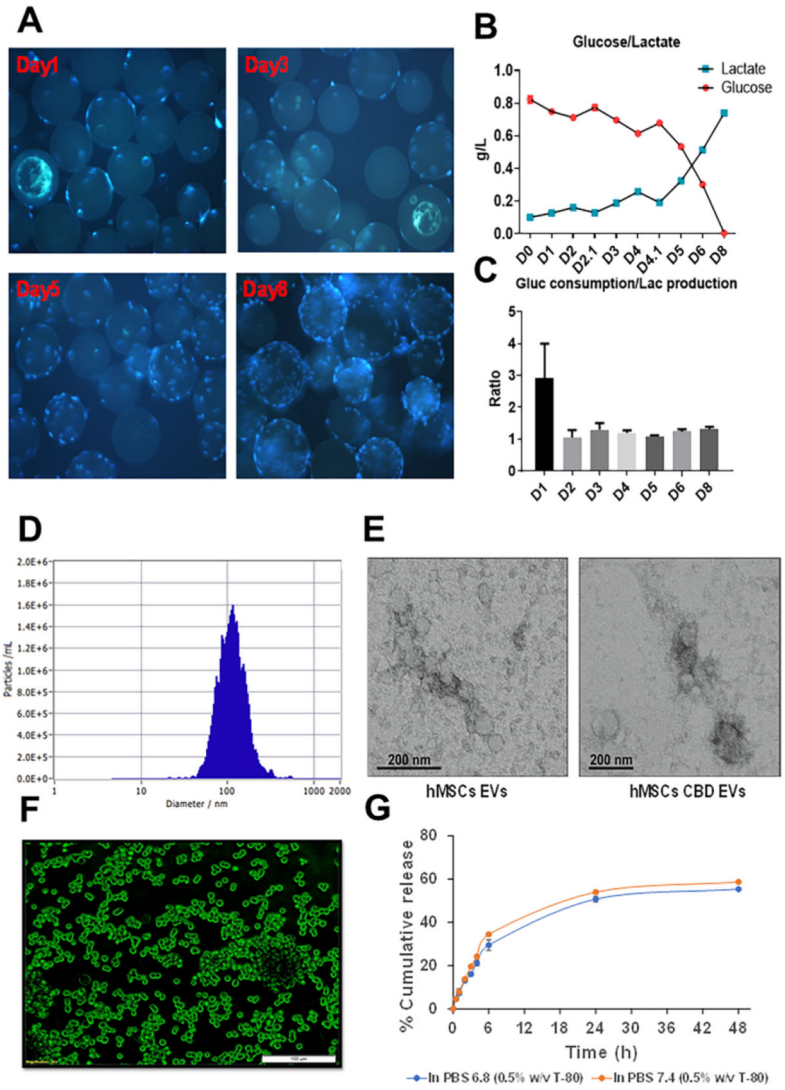

Figure 2:

Cytotoxicity assay in MDA-MB-231 cells: A. % cell inhibition with CBD at different concentrations. B. % cell inhibition with DOX at different concentrations. C.% cell inhibition with blank EVs at different particles concentration in 2D cell cultures. D. % cell inhibition with CBD EVs at different concentrations. E. % cell inhibition with CBD at different concentrations in 3D cell cultures. F. % cell inhibition with presensitization of 1 μM CBD in combination with DOX at different concentrations. G. % cell inhibition with presensitization of 1 μM CBD EVs in combination with DOX at different concentrations.

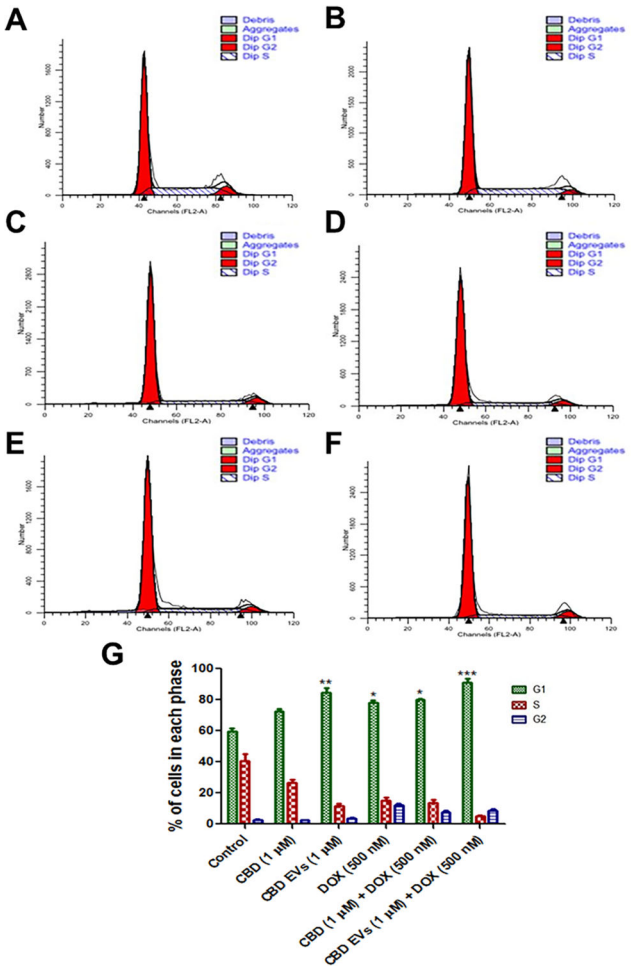

Figure 3:

Flow cytometry of cell cycle analysis. A. Representation of the flow histograms of A. CBD, B. CBD 1 μM, C. CBD EVs 1 μM, D. DOX, E. CBD + DOX, F. CBD EVs + DOX. B. Bar graphs showing cell cycle analysis after staining with propidium iodide (PI) in MDA-MB-231 cells treated with five different treatments and compared to control. All values are expressed as mean ± SEM (n=3). *p<0.05, ***p < 0.001 vs Control.

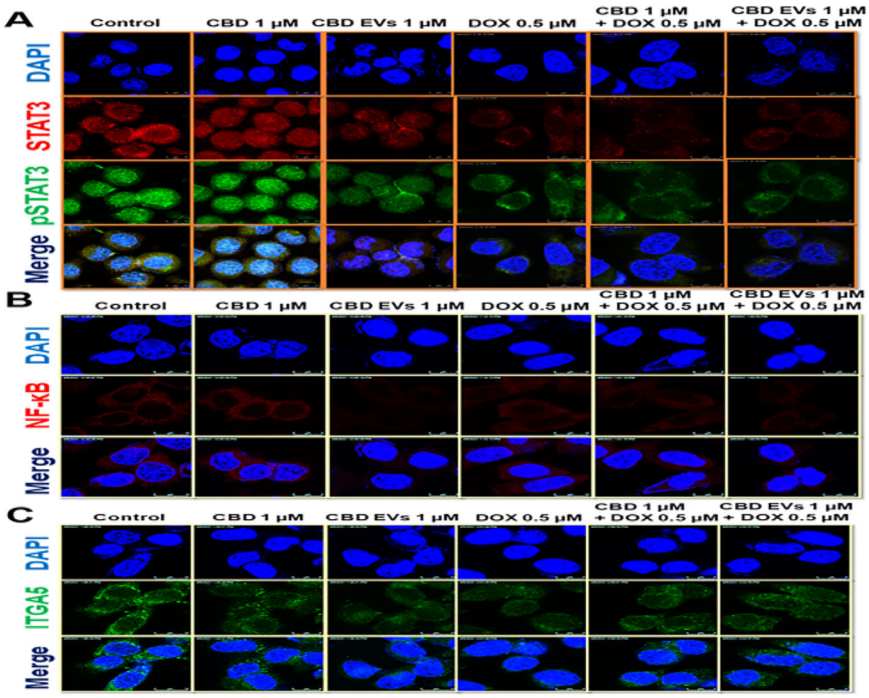

Figure 4:

Effect of CBD loaded EVs on the expression of proteins involved in Inflammation, Metastasis and Apoptosis in MDA-MB-231 cells. A. Western blots and densitometric analysis of IL-17, NF-ᴋB, Twist, P-STAT3/STAT3 proteins with free CBD and CBD EVs formulation treated MDA-MB-231 cells after 48 h. B. Western blots and densitometric analysis of BAX, Bcl2, IL-17, Twist, P-STAT3/STAT3 proteins in MDA-MB-231 cells after 48 h drug treatment with DOX alone, free CBD + DOX combination, and CBD EVs formulation + DOX. Data presented as means ± SEM, one-way ANOVA, *P<0.05, **P<0.01, ***P<0.001 significant vs control.

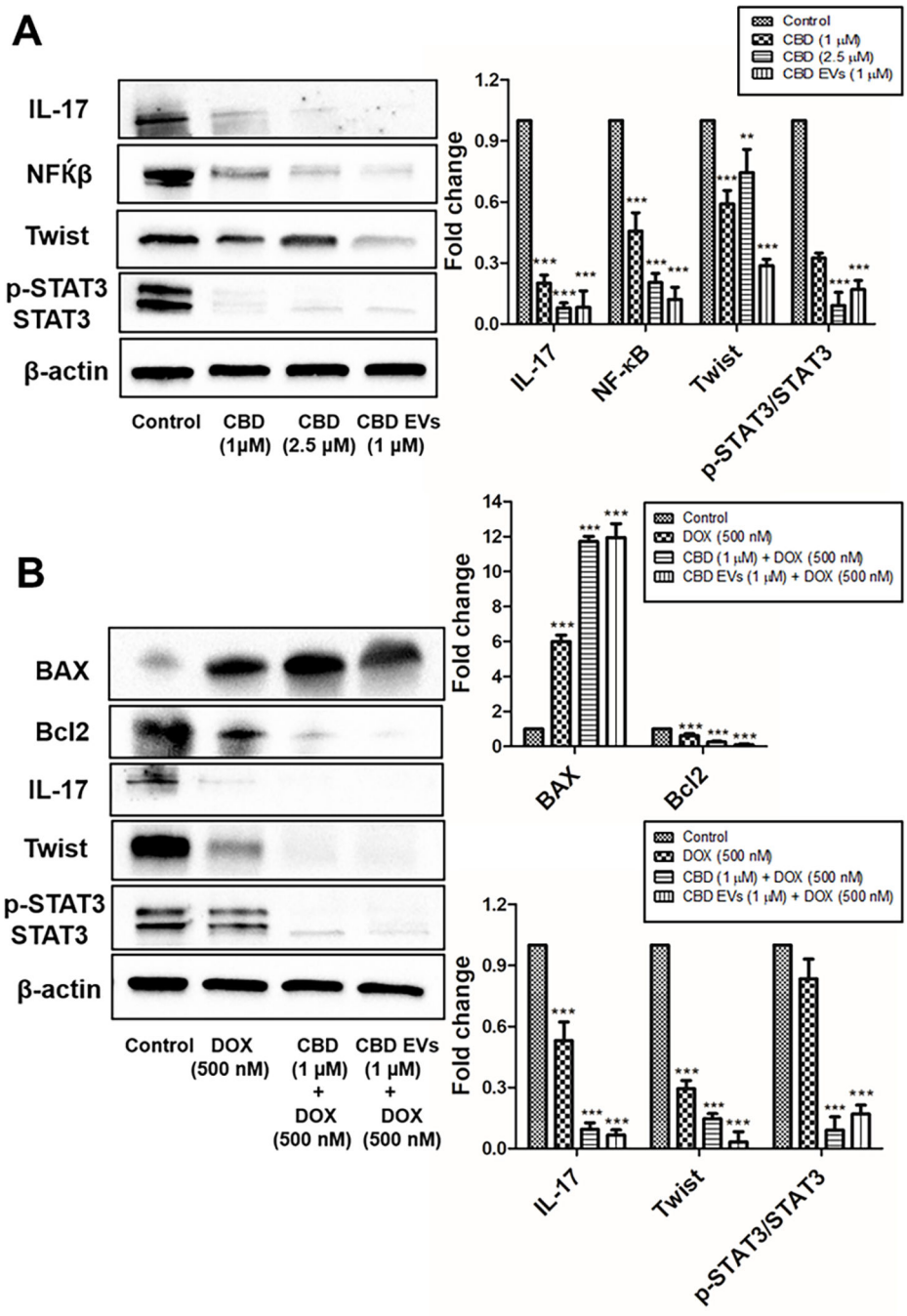

Figure 5:

Effect of CBD loaded EVs on the expression of proteins involved in inflammation, migration and invasion in MDA-MB-231 cells. A. Immunocytochemical analysis of p-STAT3& STAT3 in MDA-MB-231 cells treated with different drug treatments for 48 h. B. Immunocytochemical analysis of NF-κB in MDA-MB-231 cells treated with different drug treatments for 48 h. C. Immunocytochemical analysis of ITGA5 in MDA-MB-231 cells treated with different drug treatments for 48 h.

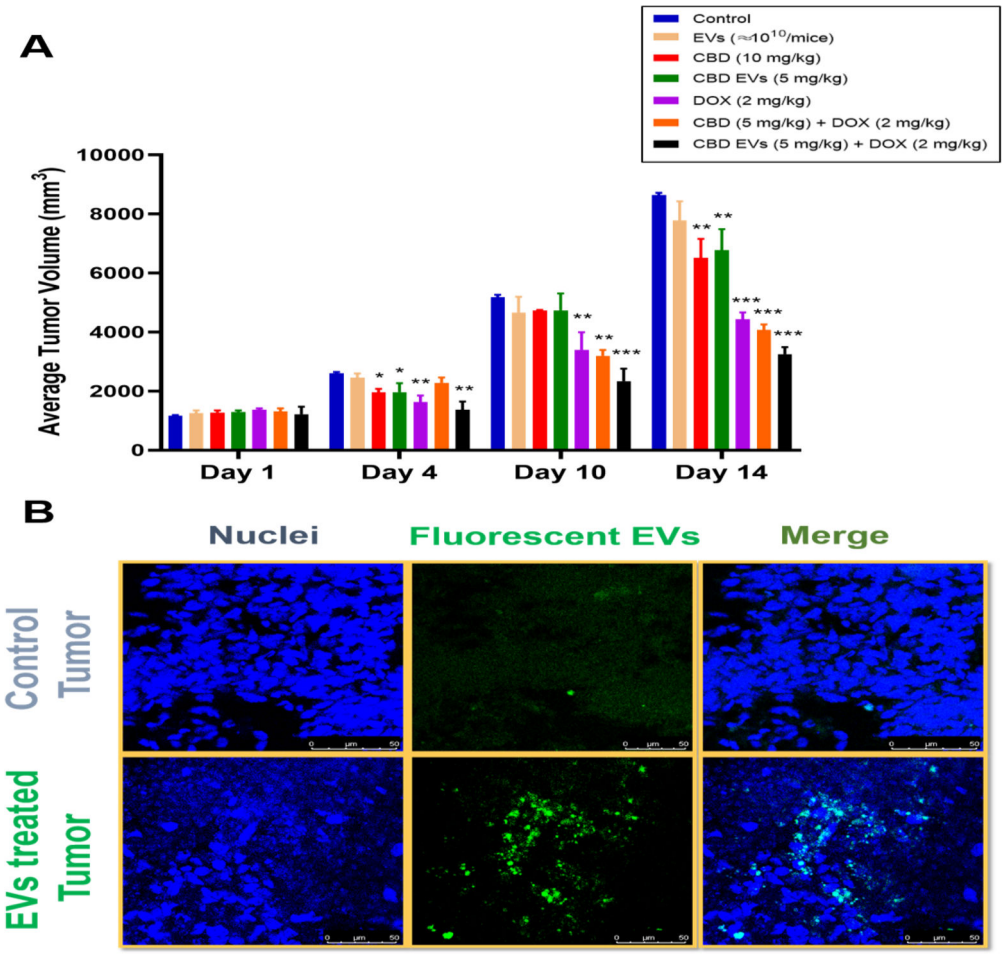

Figure 6:

In vivo anti-tumor efficacy of CBD EVs formulation + DOX combination. A. Tumor volume. B. Tumor uptake studies for Fluorescent EVs. Data presented as means ± SEM, one-way ANOVA, *P<0.05, **P<0.01, ***P<0.001 significant vs control (n=4). Control group (animals did not receive fluorescent EVs), EVs treated tumor animals (mice received fluorescent EVs at 1×10^{11} particles/mL).

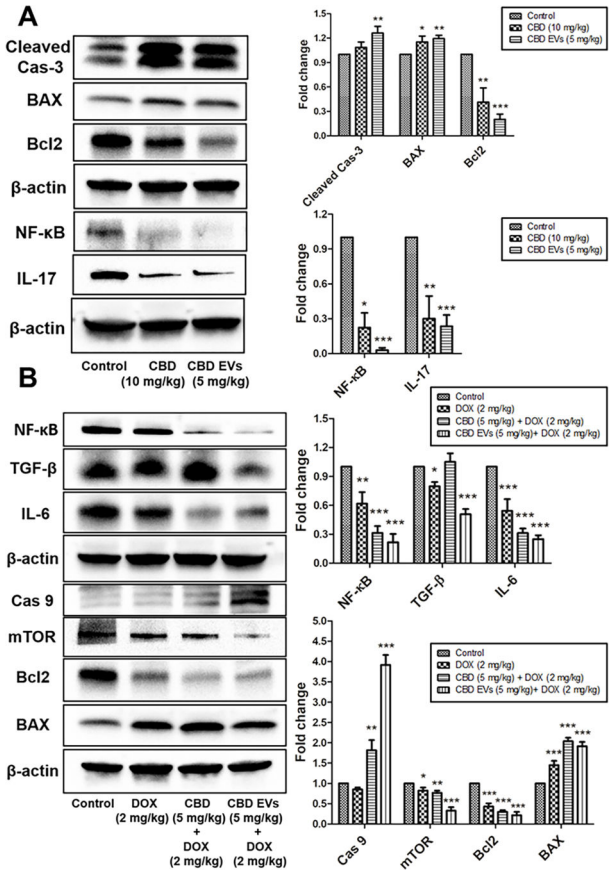

Figure 7:

Effect of CBD EVs formulation on Apoptotic and Inflammatory markers in MDA-MB-231 Triple-Negative Breast cancer Xenograft Model. A. Western blots and densitometric analysis of IL-17, NF-κB, Bcl2, BAX, Cleaved Cas-3 proteins in tumor tissue after drug treatment with CBD and CBD loaded EVs. B. Western blot and densitometric analysis of NF-κB, TGF-β, IL-6, Caspase 9, mTOR, Bcl2, BAX proteins in tumor tissue after drug treatment with DOX alone, free CBD + DOX combination, and CBD EVs formulation + DOX. Data presented as means ± SEM, one-way ANOVA, *P<0.05, **P<0.01, ***P<0.001 significant vs control.

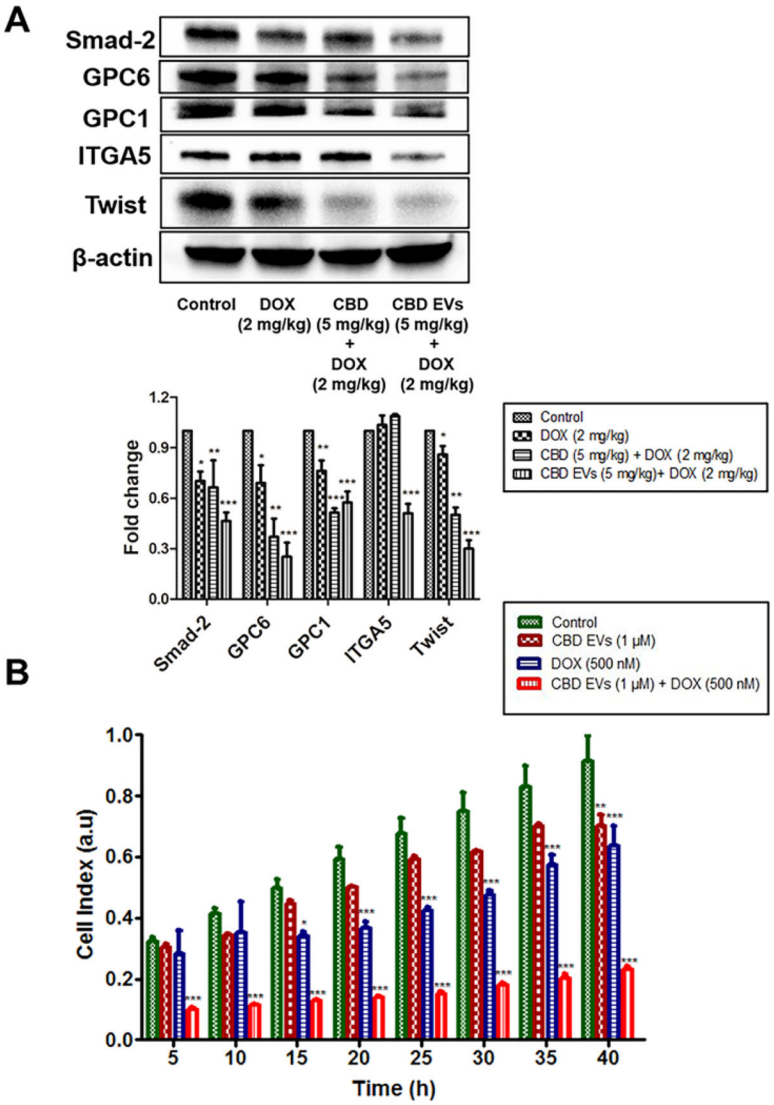

Figure 8:

CBD EVs formulation increased the sensitization of DOX in MDA-MB-231 cells *in vitro* and MDA-MB-231 xenograft model of TNBC. A. Western blots and densitometric analysis of Smad-2, GPC 6&1, ITGA5, Twist proteins in tumor tissue after drug treatment with DOX alone, free CBD + DOX combination, and CBD EVs formulation + DOX. B. Effect of CBD EVs and DOX combination on the migration of MDA-MB-231 cells. DOX (500 nM), CBD EVs (1 μM) and CBD EVs (1 μM) + DOX (500 nM) combination treated MDA-MB-231 cells were seeded in an xCelligence CIM-16 plate, and migration of the cells was monitored for 40 h and finally compared to untreated MDA-MB-231 cells; a.u, arbitrary units. Data presented as means ± SEM, one-way ANOVA, *P<0.05, **P<0.01, ***P<0.001 significant vs control.

Table 1:

Optimization parameters for the development of CBD loaded EVs

Optimization Parameters	Variable Conditions	Stability on storage at 4 °C
Buffer and pH Condition	PBS (6.8)	Unstable (Precipitation)
	PBS with 0.1 % (w/v) BSA (6.8)	Unstable (Precipitation)
	PBS (7.4)	Unstable (Precipitation)
	PBS with 0.1 % (w/v) BSA (7.4)	**Stable**
Sonication cycles	10 % Amp, 3 cycles of 30 s on/off for 2 min, 5 min-cooling between each cycle	Unstable (precipitation)
	20 % Amp, 3 cycles of 30 s on/off for 2 min, 5 min-cooling between each cycle	**Stable**
	30 % Amp, 3 cycles of 30 s on/off for 2 min with a 5 min-cooling between each cycle	Unstable (aggregation)
% CBD Loading	10	**Stable**
	20	Unstable
Incubation temperature	22/37 °C	**Stable**
Optimized formulation of CBD loaded EVs	Buffer: PBS with 0.1 % (w/v) BSA (7.4), Sonication: 20 % Amp, 3 cycles of 30 s on/off for 2 min, 5 min-cooling between each cycle, % CBD Loading: 10% w/w, Incubation temperature: 37 °C	**Stable optimized formulation**